

The Long Non-coding RNA TMPO-AS1 Promotes Bladder Cancer Growth and Progression via OTUB1-induced E2F1 Deubiquitination

Yeyu Zhang

Central South University Third Xiangya Hospital

Yuxing Zhu

Central South University Third Xiangya Hospital

Mengqing Xiao

Central South University Third Xiangya Hospital

Yaxin Cheng

Central South University Third Xiangya Hospital

Dong He

Hunan Provincial People's Hospital Department of Neurology

Jianye Liu

Central South University Third Xiangya Hospital

Liang Xiang

Central South University Third Xiangya Hospital

Lian Gong

Central South University Third Xiangya Hospital

Zhanwang Wang

Central South University Third Xiangya Hospital

Liping Deng

Central South University Third Xiangya Hospital

Ke Cao (✉ csucaoke@163.com)

Department of Oncology, The Third Xiangya Hospital of Central South University, Changsha 410013, China.

Research

Keywords: Long non-coding RNA, bladder cancer, TMPO-AS1, E2F1, OTUB1, loop

Posted Date: September 15th, 2020

DOI: <https://doi.org/10.21203/rs.3.rs-74122/v1>

License: © ⓘ This work is licensed under a Creative Commons Attribution 4.0 International License.

[Read Full License](#)

1 **The long non-coding RNA TMPO-AS1 promotes bladder**
2 **cancer growth and progression via OTUB1-induced E2F1**
3 **deubiquitination**

4

5 Yeyu Zhang¹, Yuxing Zhu¹, Mengqing Xiao¹, Yaxin Cheng¹, Dong He²,
6 Jianye Liu³, Liang Xiang¹, Lian Gong¹, Zhanwang Wang¹, Liping Deng¹,
7 Ke Cao^{1, *}

8

9 ¹Department of Oncology, The Third Xiangya Hospital of Central South
10 University, Changsha 410013, China.

11 ²Department of Respiratory, The Second People's Hospital of Hunan
12 Province, Changsha 410007, China.

13 ³Department of Urology, The Third Xiangya Hospital of Central South
14 University, Changsha 410013

15

16 Correspondence to: Ke Cao, Department of Oncology, The Third
17 Xiangya Hospital, Central South University, 138 Tongzipo Road,
18 Changsha 410013, China

19 Email: csucaoke@163.com

20 Tel: +86 0731-88618240

21 Fax: +86 0731-88618285

22 **Abstract**

23 **Background**

24 Bladder cancer (BC) is the most common malignant tumor of the urinary
25 system. Increasing evidence indicates long non-coding RNAs (lncRNAs)
26 play crucial roles in cancer tumorigenesis, development, and progression.
27 However, the role of TMPO antisense RNA 1 (TMPO-AS1) is still need
28 to be explored in BC.

29 **Methods**

30 The lncRNA TMPO-AS1 expression was evaluated by bioinformatics
31 analysis and further validated by qRT-PCR. Loss- and gain-of- function
32 assays were performed to determine the biological functions of TMPO-
33 AS1 in BC proliferation, migration, and invasion. Chromatin
34 immunoprecipitation, luciferase reporter assays, western blotting, RNA
35 pull-down, RNA immunoprecipitation assays, and fluorescence in situ
36 hybridization were conducted to explore the molecular mechanisms of
37 TMPO-AS1/E2F transcription factor 1 (E2F1) loop.

38 **Results**

39 TMPO-AS1 is upregulated in bladder cancer and is associated with BC
40 patients' poor prognoses. Functional experiments demonstrated that

41 TMPO-AS1 promotes bladder cancer cell proliferation, migration,
42 invasion, and inhibits cell apoptosis *in vivo* and *in vitro*. Mechanically,
43 E2F1 is responsible for the TMPO-AS1 upregulation. Additionally,
44 TMPO-AS1 facilitates the interaction of E2F1 with OTU domain-
45 containing ubiquitin aldehyde binding 1 (OTUB1), leading to E2F1
46 deubiquitination and stabilization, thereby promotes BC malignant
47 phenotypes. Furthermore, rescue experiments showed that TMPO-AS1
48 promotes BC growth in an E2F1-dependent manner.

49 **Conclusions**

50 Our study is the first to uncover a novel positive regulatory loop of
51 TMPO-AS1/E2F1 important for the promotion of BC malignant
52 behaviors. The TMPO-AS1/E2F1 loop should be considered in the quest
53 for new BC therapeutic options.

54 **Keywords:** Long non-coding RNA, bladder cancer, TMPO-AS1, E2F1 ,
55 OTUB1, loop

56

57

58

59

60

61 **Background**

62 Bladder cancer (BC) is the most common malignant tumor of the
63 urinary system worldwide [1], 549,393 new cases and 199,922 cancer-
64 related deaths were reported in 2018 [2]. The majority of BCs are
65 urothelial cell carcinomas. Urothelial BC can be categorized into non-
66 muscle-invasive BC (NMIBC) and muscle-invasive BC (MIBC).
67 Approximately, 75% of BC patients exhibit NMIBC with high recurrence
68 and progression, while the remaining 25% of BC patients present with
69 MIBC and have a poor prognosis [3]. Although therapies including
70 transurethral resection tumor, cystectomy, chemotherapy, radiation, and
71 immunotherapy have contributed to the reduction of BC-associated
72 morbidity/mortality, the five-year survival rates of BC patients have
73 hardly improved, causing a heavy burden on the health care systems
74 worldwide [4]. Therefore, it is urgent to explore the molecular
75 mechanisms and biomarkers of BC to develop better diagnostic,
76 monitoring, and therapeutic approaches and reduce disease burden.

77 Long non-coding RNAs (lncRNAs) are a class of non-coding RNAs,
78 longer than 200 nucleotides with limited protein-coding potential [5].
79 Accumulating pieces of evidence have revealed that lncRNAs influence
80 several biological/pathological processes, such as cell proliferation,
81 metastasis, drug resistance, and metabolism, and are involved in multiple

82 diseases, particularly in cancer [6, 7, 8]. LncRNAs may be oncogenes or
83 tumor suppressors via the regulation of gene expression (e.g. epigenetic
84 regulation, transcriptional activation or repression, post-transcriptional
85 modulation), or even via protein modification [9, 10, 11]. Previous
86 studies have suggested that numerous lncRNAs are involved in BC [12,
87 13, 14]. For instance, MALAT1 promotes BC metastasis by associating
88 with suz12 [15]. FOXD2-AS1 facilitates bladder tumor growth and
89 recurrence via a positive feedback loop with Akt and E2F1 [16].
90 Moreover, recent studies have demonstrated that upregulated TMPO
91 antisense RNA 1 (TMPO-AS1) serves as competing endogenous RNA to
92 sponge microRNAs (miRNAs) in multiple carcinomas including
93 hepatocellular carcinoma, thyroid cancer, lung adenocarcinoma, and
94 breast cancer [17, 18, 19, 20]. However, whether TMPO-AS1 plays a role
95 by interacting with other molecules in BC is an interesting question
96 requiring further investigation.

97 Besides regulating mRNA transcription, transcription factors (TFs)
98 are also involved in the regulation of lncRNA transcription [21]. E2F1, a
99 member of the E2F transcription factor family consisting of eight
100 proteins, is a transcription activator essential for the regulation of cell
101 cycle, apoptosis, cell proliferation, and DNA damage response [22].
102 Studies have demonstrated that E2F1 can modulate the expression of

103 lncRNAs and coding genes [23, 24]. However, little is known on the
104 E2F1-mediated lncRNAs regulation in BC. Protein stabilization can be
105 modulated by ubiquitination and deubiquitination [25]. E2F1 was
106 reported to be stabilized via preventing its ubiquitination [26]. POH1, a
107 deubiquitinase, was reported to promote the development of liver cancer
108 via E2F1 deubiquitylation [27]. However, no lncRNAs have been linked
109 to E2F1 ubiquitination/deubiquitination.

110 Here, we focus on the roles of TMPO-AS1 in BC carcinogenesis and
111 investigate the upstream and downstream regulations of TMPO-AS1. We
112 demonstrate that E2F1 activates TMPO-AS1 transcription, on the other
113 hand, TMPO-AS1 facilitates the interaction of E2F1 with OTUB1, a
114 deubiquitinase, and consequently increases E2F1 protein levels via
115 stabilization, promoting BC malignant phenotypes. Therefore, the
116 TMPO-AS1/E2F1 positive feedback loop should be considered as a novel
117 target for BC.

118

119 **Materials and methods**

120 **Bioinformatics analysis**

121 The lncRNA TMPO-AS1 expression data in 33 types of human
122 cancers was obtained from the Gene Expression Display Server (GEDS)
123 [28]. TMPO-AS1 expression in BC tissues and normal tissues were

124 analyzed using The Cancer Genome Atlas (TCGA) BLCA RNA-seq data
125 retrieved from UCSC XENA (<https://xena.ucsc.edu>), TANRIC [29],
126 Gene Expression Omnibus (GEO, www.ncbi.nlm.nih.gov, GSE133624
127 and GSE120736 datasets) [30], The prognostic value of TMPO-AS1 was
128 evaluated using GEPIA 2 (<http://gepia2.cancer-pku.cn/#index>) [31].
129 hTFtarget and ChIPBase v2.0 were used to find out the potential TFs of
130 TMPO-AS1 [32, 33]; JASPAR 2018 database was utilized to identify the
131 E2F1-TMPO-AS1 binding profile [34]. Genes co-expressed with TMPO-
132 AS1 (TCGA-BLCA dataset) were defined as those with correlation
133 coefficients ≥ 0.6 and p values < 0.01 using Co-LncRNA [35]. Pathway
134 enrichment analysis was conducted using Metascape [36]. The interaction
135 of E2F1, OTUB1, and TMPO-AS1 was predicted via catRAPID [37] and
136 PRIdictor [38]. The interaction between E2F1 and OTUB1 proteins was
137 predicted using HDOCK [39]. The ubiquitination sites of E2F1 were
138 predicted using UbPred [40].

139

140 **Clinical samples**

141 Resected BC and normal adjacent specimens were collected from BC
142 patients admitted to the Third Xiangya Hospital from 2016 to 2018; all
143 patients were provided with written informed consent. Six pairs of BC
144 and paired adjacent normal tissues were stored in liquid nitrogen at -80

145 °C. This study was approved by the ethics committee of the Third
146 Xiangya Hospital, Central South University.

147

148 **Cell culture and treatment**

149 The human bladder cell lines BIU87, 5637, T24, EJ, and RT4 were
150 obtained from American Type Culture Collection (ATCC) (Rockville,
151 MD, USA). Cells were cultured in DMEM (Invitrogen, Carlsbad, CA,
152 USA) medium containing 10% fetal bovine serum (FBS) (Gibco, Thermo
153 Fisher Scientific, Waltham, MA, USA), 1 mmol/L glutamine and 100
154 U/mL penicillin/, at 37°C in an incubator with 5% CO₂. Protein synthesis
155 inhibitor cycloheximide (10 µg/ml, Millipore, Sigma, C1998) and
156 proteasome inhibitor MG132 (20 µM, Selleck, S2619) were used to
157 examine ubiquitin proteasome-related protein degradation.

158

159 **Quantitative real-time PCR**

160 Total RNA was extracted from the BC tumor tissues, the paired
161 adjacent normal tissues, and BC cells (T24 and RT4) using TRIzol
162 (Invitrogen, , Carlsbad, CA, USA) according to the manufacturer's
163 instructions. The PrimeScript RT Reagent Kit (TaKaRa, Dalian, China)
164 was used to synthesize complementary DNAs (cDNAs). qRT-PCR was
165 performed using the SYBR Green PCR Master Mix (Toyobo, Osaka,

166 Japan), as per the manufacturer's instructions. β -actin and GAPDH
 167 served as the internal references. The $2^{-\Delta\Delta CT}$ method(Ct, cycle threshold)
 168 was applied to determine the relative gene expression. All experiments
 169 were performed in triplicate. The primer sequences used in this study are
 170 listed in Table 1.

Table 1. Primers used for qRT-PCR, siRNAs oligonucleotides, and ChIP

Primers used for qRT-PCR		
	TMPO-AS1-F	AGAGCCGAACTACGAACCAA
	TMPO-AS1-R	CTGTCCCTTATCGGCGTCT
	E2F1-F	ACGTGACGTGTCAGGACCT
	E2F1-R	GATCGGGCCTTGTTTGCTCTT
	β -actin-F	CATGTACGTTGCTATCCAGGC
	β -actin-R	CTCCTTAATGTCACGCACGAT
	U1-F	GGGAGATAACCATGATCACGAAGGT
	U1-R	CCACAAATTATGCAGTCGAGTTTCCC
siRNAs oligonucleotides		
	TMPO-AS1-F	GAGCCGAACUACGAACCAACU
	TMPO-AS1-R	UUGGUUCGUAGUUCGGCUCUG
	E2F1	ACCTCTTCGACTGTGACTTTG
	OTUB1-F	AGCGACUCCGAAGGUGUUAAC
	OTUB1-R	GUUAACACCUUCGGAGUCGCU
	Negative control-F	UUCUCCGAACGUGUCACGUTT
	Negative control-R	ACGUGACACGUUCGGAGAATT
ChIP		
	TMPO-AS1-F	CAACAAGTGC GACTCCAT
	TMPO-AS1-R	GTGTGGAGGGCTTTTTGAAC
	GAPDH-F	TACTAGCGGTTTTACGGGCG
	GAPDH-R	TCGAACAGGAGGAGCAGAGAGCGA

171

172 Cell transfection

173 For *in vitro* function assays, TMPO-AS1-targeted, E2F1-targeted, and
 174 OTUB1-targeted small interfering RNAs(si-TMPO-AS1, si-E2F1, si-
 175 OTUB1), and overexpression plasmids for TMPO-AS1 and E2F1(OE-

176 TMPO-AS1, OE-E2F1) as well as the empty vectors were purchased
177 from GeneChem Co. (Shanghai, China) and transfected into T24 and RT4
178 cells using the Lipofectamine 3000 Reagent (Invitrogen Carlsbad, CA).
179 For *in vivo* xenograft experiments, RT4 cells were stably transfected with
180 the empty lentiviral vectors, sh-TMPO-AS1(designed according to si-
181 TMPO-AS1), or sh-TMPO-AS1 together with E2F1 expressing lentiviral
182 vectors purchased from GeneChem (Shanghai, China) according to
183 manufacturers' protocol. The empty vector was used as the negative
184 control. The transfection efficiency was determined via qRT-PCR.

185

186 **Methyl thiazolyl tetrazolium (MTT) assay**

187 The MTT assay was conducted according to the manufacturer's
188 instructions. The BC cells were inoculated in 96-well plates at a density
189 of 1×10^4 cells/well and incubated for 24 h. Next, 10 μ l of MTT solution
190 (Sigma Chemicals, St. Louis, MO, USA) was added to each well and
191 cells were cultured at 37°C for 4 h. Next, cell viability/proliferation was
192 estimated via measuring the absorbance at 570 nm with the Epoch
193 Microplate Spectrophotometer (BioTek Instruments, Winooski, VT,
194 USA).

195

196 **Colony formation assay**

197 Colony formation assay was performed as previously described [41].
198 BC cell proliferation was evaluated using colony formation assay.
199 Briefly, T24 and RT4 cells, treated as described above, were seeded into
200 6-well plates at a density of 1000 cells/well and cultured for 2-3 weeks.
201 Then, cells were washed with FBS, fixed with 4% paraformaldehyde,
202 stained with 1% crystal violet, and counted (more than 50 cells).

203

204 **Cell apoptosis analysis**

205 Cell apoptosis in BC cells (T24 and RT4 cells) was investigated via
206 flow cytometry using the Annexin V-PE/7-AAD kit
207 (KA3809, Abnova, Wuhang, China), according to the manufacture's
208 protocol.

209

210 **Wound healing assay**

211 A wound healing assay was conducted as previously described [42].
212 Briefly, cells were seeded into 6-well plates at a density at 1×10^5
213 cells/well. Then, a sterile 200 μ l pipette tip was used to scratch a straight
214 line in the cell monolayer. Next, cells were washed with FBS and
215 cultured for 48 h. The scratch width was measured 48 h later.

216

217 **Transwell assay**

218 Transwell assay was conducted to evaluate cell migration and
219 invasion. 5×10^4 BC cells (T24 and RT4) were suspended in serum-free
220 medium and seeded into the upper chamber of 8 μm pores (Corning,
221 Corning, NY, USA) with Matrigel (BD Biosciences, San Jose, CA, USA)
222 while complete medium with 10% FBS was added to the lower chamber.
223 After 48-h incubation, the migrating cells were fixed with 4%
224 paraformaldehyde, stained with 0.1% crystal violet (Sigma-Aldrich, St.
225 Louis, MO, USA), photographed under a microscope (DMB5-2231P1,
226 Hong Kong, China).

227

228 **Western blotting**

229 Total protein was extracted using RIPA buffer (Beyotime, Shanghai,
230 China) with a protease inhibitor cocktail (Roche, Basel Switzerland).
231 Protein concentration was measured using a BCA kit (Thermo Fischer
232 Scientific, Waltham, MA, USA). Protein samples were resolved via SDS-
233 PAGE and transferred onto PVDF membranes. Next, the membranes
234 were blocked in PBS containing 5% skim milk powder at room
235 temperature for 1 h, and incubated with the primary antibodies at 4°C
236 overnight, followed by the secondary antibodies. The protein bands were
237 visualized using the Pierce® ECL Western Blotting Substrate kit

238 (32106; Thermo Scientific), and normalized by β -actin as reference. The
239 antibodies used in this study were listed in Additional file 1: Table S1

240

241 **Luciferase reporter assay**

242 The wild-type or mutant-type of E2F1 binding sites to the promoter of
243 TMPO-AS1 were synthesized and inserted into pGL3 vector (Promega,
244 Madison, WI, USA), respectively. T24 and RT4 cells were seeded into
245 48-well plates and co-transfected with the above vectors along with E2F1
246 expression or control plasmids. Forty-eight hours later, the luciferase
247 activity was measured and analyzed using the Luciferase Reporter Assay
248 System (Promega).

249

250 **Chromatin immunoprecipitation assay**

251 Chromatin immunoprecipitation (ChIP) assay was performed using
252 the EZ Magna ChIP™ kit (Millipore, Burlington, MA, USA) according
253 to the manufacturers' instructions. Briefly, 1×10^7 cells (T24 and RT4)
254 were fixed with 1% formaldehyde and treated with 10% glycine. Next,
255 the cross-linked chromatin was broken into small DNA fragments via
256 sonication. The sonicated DNA was immunoprecipitated using antibodies
257 against E2F1 and control rabbit IgG (Bioss Antibodies Inc., Woburn,

258 MA, USA). qRT-PCR was performed to quantify the precipitated
259 chromatin using the specific primers. The primers are listed in Table 1.

260

261 **RNA pull-down assay**

262 TMPO-AS1 was transcribed *in vitro* and labeled with 3' end
263 biotinylation. The RNA pull-down assay was performed using the
264 Pierce™ Magnetic RNA-Protein Pull-Down Kit (Thermo Fischer
265 Scientific, Waltham, MA, USA). Briefly, the lysates of control or TMPO-
266 AS1 overexpressing T24 and RT4 cells were incubated with control or
267 biotinylated TMPO-AS1 at room temperature for 4h, followed by
268 addition with streptavidin magnetic beads (Thermo Fisher, USA) at 4°C
269 for 60 min with rotation. After three washing steps with washing buffer,
270 the RNA-binding proteins were eluted using 50 µl elution buffer and
271 analyzed via western blotting.

272

273 **RNA immunoprecipitation (RIP)**

274 RIP was performed using the EZ-Magna RIP™ RNA-Binding Protein
275 Immunoprecipitation Kit (Millipore, Burlington, MA, USA) based on
276 the manufacturer's instructions. Cell extracts were incubated with
277 magnetic beads conjugated with antibodies against SNRNP70
278 (Cat.#CS203216), normal rabbit IgG(Cat.#PP64B), and anti-E2F1

279 (Cat.#OM250777). were used as positive and negative controls. Anti-
280 SNRNP70 antibody was used as positive control, whereas normal rabbit
281 IgG was used as a negative control. The relative abundance of TMPO-
282 AS1 was normalized to the amount of enriched U1snRNA via qRT-PCR.

283

284 **Co-immunoprecipitation (Co-IP)**

285 Cell lysates were incubated with primary antibody against E2F1
286 (1:80, OM250777, Omnimabs) at 4°C overnight. The rabbit IgG antibody
287 (1:150, Bioss Antibodies Inc., Woburn, MA, USA) was used as a
288 negative control. Next, cell lysates were mixed with protein A/G agarose
289 (Cat. #P1012, Beyotime Biotechnology) at 4°C for 2 h, followed by
290 centrifugation and washing steps. The precipitated complex was
291 separated using SDA-PAGE and analyzed via western blotting.

292

293 **Fluorescence in situ hybridization (FISH)**

294 FISH assay was performed using Ribo™ Fluorescent in Situ
295 Hybridization (RiboBio, Guangzhou, China) following the
296 manufacturer's instructions. TMPO-AS1 and 18S probes were
297 synthesized and labeled with Cy3 fluorescent dye. Fluorescence was
298 detected under a confocal laser microscope (Leica, SP5).

299

300 **Immunohistochemistry (IHC)**

301 IHC staining was performed as previously described[43]. Tissues
302 sections obtained from paraffin-embedded tissues were dewaxed in
303 xylene and rehydrated in an ethanol gradient. Next, tissues were
304 incubated in 1 % hydrogen peroxide and boiled in citrate buffer (10
305 mM, pH=6.0) for 15 min. Subsequently, tissues were incubated with the
306 primary antibodies against Ki-67 (1:1000;27309-1-AP, Proteintech,
307 Chicago, IL, USA), E2F1 (1:200, OM250777, Omnimabs), and caspase-
308 3(1:200,19677-1-AP, Proteintech) at 4°C overnight, followed by
309 incubation with HRP-conjugated goat anti-rabbit secondary antibody.
310 (SP-9000, zsbio, Beijing, China) at room temperature for 30 min.
311 Diaminobenzidine was used for chromogen; hematoxylin was used as the
312 nuclear counterstain.

313

314 **Xenograft mouse model**

315 The experiments were approved by the Animal Care and Use
316 Committee of the Central South University. 1×10^6 RT4 cells transfected
317 with the empty, TMPO-AS1 knockout, or depletion of TMPO-AS1
318 coupled with E2F1 lentiviral vectors were injected subcutaneously into
319 the flanks of male BALB/c nude mice (4- to 6-week-old, n=4 per group)
320 obtained from the Shanghai Experimental Laboratory Animal Center

321 (Shanghai, China). Tumor volumes were measured every 3 days and
322 calculated as follows: tumor volume = $(D \times d^2)/2$, where D and d refer to
323 the longest and shorter diameters, respectively. Mice were euthanized
324 after twenty-five days.

325

326 **Statistical analysis**

327 All statistical analyses were performed using the GraphPad Prism
328 software, version 8 (GraphPad Software, San Diego, CA, USA). Data are
329 presented as the mean \pm SD of at least three independent experiments.

330 The relationship between E2F1 and TMPO-AS1 was analyzed using the
331 Pearson correlation coefficient. Significant differences were analyzed
332 using Student's t-test or the one-way analysis of variance (ANOVA). P
333 <0.05 was considered statistically significant.

334

335 **Results**

336 **TMPO-AS1 is upregulated in BC tissues and is associated with** 337 **Poor Prognosis**

338 To evaluate TMPO-AS1 expression in tumor and normal tissues, we
339 used the online database GEDS and found that TMPO-AS1 expression is
340 upregulated in multiple tumor tissues compared with that in normal
341 tissues (Fig. 1a). Consistently, the expression of TMPO-AS1 was

342 upregulated in BC tissues compared with the normal tissues according to
343 TCGA (Fig. 1b) and TANRIC databases (Fig. 1c). We further confirmed
344 that TMPO-AS1 expression was higher in six paired BC tissues
345 compared with the corresponding normal tissues via qRT-PCR (Fig. 1d).
346 Moreover, the integrative analysis of GSE133624 and GSE120736
347 showed that TMPO-AS1 was not only highly expressed in BC tissues
348 (Fig. 1e) , but also exhibited higher levels in MIBC *versus* NMIBC
349 samples (Fig. 1f). Of note, higher expression of TMPO-AS1 was
350 associated with BC recurrence (Fig. 1g), and advanced tumor stage
351 (Additional file 2: Figure S1). Furthermore, BC patients with higher
352 TMPO-AS1 expression levels were associated with shorter disease-free
353 survival time (Fig. 1h). Taken together, these data suggest that TMPO-
354 AS1 is highly expressed in BC tissues and is associated with poor
355 prognosis.

356

357 **TMPO-AS1 promotes cell proliferation, migration, and invasion** 358 **of BC cells, and survival *in vitro*.**

359 Since TMPO-AS1 expression was the highest in T24 and RT4 cells
360 among five BC cell lines (BIU87, 5637, T24, EJ, and RT4) using qRT-
361 PCR (Fig. 2a), they were selected for following experiments. To
362 investigate the functions of TMPO-AS1, si-RNA targeting TMPO-AS1

363 and expression plasmid of TMPO-AS1 were transfected into T24 and
364 RT4 cells. As shown in Fig. 2b, the transfection efficacy was examined
365 using qRT-PCR. Next, loss- and gain-of-function assays were performed.
366 The results showed that knockdown of TMPO-AS1 significantly
367 inhibited cell viability/proliferation (Fig. 2c, d) , migration (Fig. 2e), and
368 invasion (Fig. 2f), while TMPO-AS1 overexpression resulted in the
369 opposite effects. Additionally, cell apoptosis was induced in TMPO-AS1-
370 silenced T24 and RT4 cells, whereas overexpression of TMPO-AS1
371 inhibited cell apoptosis (Fig. 2g). Overall, these findings suggest that
372 TMPO-AS1 plays an oncogenic role in BC cells, promoting their
373 proliferation, migration, invasion, and survival *in vitro*.

374

375 **E2F1 activates the transcription of TMPO-AS1 in BC cells**

376 To figure out the underlying mechanism of TMPO-AS1-mediated
377 carcinogenic properties in BC, we investigate the upstream and
378 downstream genes of TMPO-AS1. Previous studies have revealed that
379 TFs can serve as the upstream genes of lncRNAs and regulate their
380 transcription [21, 44]. Therefore, we screened out the potential TFs of
381 TMPO-AS1 using hTF target and CHIP base V2.0 (Fig. 3a, Additional
382 file 3: Table S2). We obtained 36 candidate TFs for TMPO-AS1, Of note,
383 E2F1 had the highest positive correlation with TMPO-AS1 among 36

384 TFs. (Additional file 3: Table S2). Importantly, a previous study reported
385 that the overexpression of E2F3 induced the promoter activity of TMPO-
386 AS1/LAP2, an antisense transcript [45]. Meanwhile, we analyzed genes
387 co-expressed with TMPO-AS1 (correlation coefficient ≥ 0.6 and p value
388 < 0.01) in BC using Co-LncRNA (Additional file 4: Table S3).

389 Additionally, we performed pathway analysis of TMPO-AS1-associated
390 genes via Metascape and found that TMPO-AS1 is involved in the E2F
391 pathway (Fig. 3b). Thus, we focused on E2F1 in the following research.
392 E2F1 was positively correlated with TMPO-AS1 in BC as evidenced by
393 TCGA and GSE133624 datasets (Fig. 3c, d). Furthermore,
394 the expression of TMPO-AS1 was downregulated after E2F1 silencing,
395 while upregulated in E2F1 overexpressing BC cells (Fig. 3e). The
396 putative binding sites between TMPO-AS1 and E2F1 were at -945 ~ -935
397 bp upstream transcription start site as predicted by JASPAR(Fig. 3f). As
398 expected, overexpression of E2F1 dramatically enhanced the luciferase
399 activity of wild-type TMPO-AS1 promoter, whereas E2F1 failed to alter
400 the transcriptional activity of mutant TMPO-AS1 promoter (Fig. 3g).

401 Moreover, the results of ChIP assay demonstrated that E2F1 was
402 remarkably enriched in TMPO-AS1 promoter region relative to the
403 control IgG (Fig. 3h). Overall, these results indicate that E2F1 can bind to
404 the promoter of TMPO-AS1 and activate its transcription.

405 **TMPO-AS1 regulates E2F1 protein levels via protein**
406 **stabilization**

407 Given that lncRNAs have been reported to interact with E2F1 [46,
408 47], we then investigate whether TMPO-AS1 could interact with E2F1.
409 As shown in Fig. 4a, a possible interaction between TMPO-AS1 and
410 E2F1 was predicted by catRAPID. Consequently, we conducted RNA
411 pull-down assays to validate the prediction. The results showed that E2F1
412 was abundantly enriched by TMPO-AS1 probe compared with the control
413 oligo, especially in TMPO-AS1 overexpressing RT4 and T24 cells (Fig.
414 4b). Similarly, RIP results demonstrated that E2F1 remarkably
415 immunoprecipitated TMPO-AS1, which was enhanced upon TMPO-AS1
416 overexpression in RT4 and T24 cells (Fig 4c). The interaction between
417 TMPO-AS1 and E2F1 prompted us to investigate whether TMPO-AS1
418 influenced the expression of E2F1. Interestingly, overexpression or
419 knockdown of TMPO-AS1 had no significant impact on *E2F1* mRNA
420 expression (Fig. 4d), while notably increased or decreased E2F1 protein
421 expression in RT4 and T24 cells (Fig. 4e), respectively, suggesting
422 TMPO-AS1-mediated E2F1 regulation occurs at the post-transcriptional
423 level. Then, we found that proteasome inhibitor MG132 markedly
424 increased the stability of E2F1 protein in cycloheximide-treated RT4 and
425 T24 cells (Fig. 4f), implying the turnover of E2F1 was subjected to

426 ubiquitin proteasome system. Importantly, silencing TMPO-AS1
427 significantly shortened the half-life of E2F1 (Fig. 4g) Altogether, our data
428 demonstrate that TMPO-AS1 directly interacts with E2F1 and regulates
429 its protein levels via protein stabilization.

430

431 **TMPO-AS1 stabilizes E2F1 via OTUB1-mediated** 432 **deubiquitination**

433 To investigate the underlying mechanism of TMPO-AS1-mediated
434 E2F1 stabilization. Firstly, we performed FISH assay and found that
435 TMPO-AS1 is predominantly distributed in the cytoplasm in both T24
436 and RT4 cells (Fig. 5a), indicating TMPO-AS1 might involve in
437 translational regulation. It has been proposed that POH1 (PSMD14), a
438 deubiquitinase, binds to and deubiquitilates E2F1 protein, which
439 contributes to E2F1 stabilization, thereby promotes liver cancer
440 development[27]. Moreover, it was predicted that E2F1 has four potential
441 ubiquitination sites by UbPred (Additional File 5: Fig S2A). Therefore,
442 we hypothesized that TMPO-AS1 may associate with a specific
443 ubiquitinase/deubiquitinase to regulate E2F1 ubiquitination. Since we
444 have studied a group of deubiquitinases (OTUB1, UCHL5, USP5,
445 COPS6, and PSMD14) in BC (unpublished data), we concentrated on

446 deubiquitinases in the following studies. We evaluated the binding
447 potential of the above deubiquitinases to TMPO-AS1 using PRIdictor.
448 The results highlighted OTUB1, as the deubiquitinase that most likely
449 associates with TMPO-AS1(Additional File 5: Fig S2 B). To validate the
450 prediction, we conducted RNA pull-down assays and found that TMPO-
451 AS1 precipitated more OTUB1 than the other deubiquitinases (Fig. 5b).
452 Similarly, RIP assays showed that TMPO-AS1 was obviously
453 immunoprecipitated by the anti-OTUB1 antibody compared with IgG
454 (Fig. 5c). Furthermore, CatRAPID showed that the region of TMPO-AS1
455 at 76-127 nucleotides exhibits a high potential of interaction with the
456 OTUB1 amino acid residues at 51-152 (Additional File 5: Fig S2C),
457 further supporting the association between TMPO-AS1 and OTUB1.
458 Despite the direct association between TMPO-AS1 and OTUB1, TMPO-
459 AS1 failed to alter OTUB1 protein expression (Fig. 5d). Obviously,
460 OTUB1 knockdown led to a decrease in E2F1 protein levels in RT4 and
461 T24 cells(Fig. 5e). In addition, as per HDock prediction, OTUB1 was
462 very likely to bind to E2F1 (Fig. 5f). Importantly, the results of Co-IP
463 assays showed that silencing TMPO-AS1 not only increased E2F1
464 ubiquitination, but also mitigated the interaction between OTUB1 and
465 E2F1(Fig. 5g), which could be rescued by overexpression of TMPO-AS1.
466 Furthermore, knockdown of OTUB1 significantly reversed the decreased

467 ubiquitination of E2F1 induced by overexpression of TMPO-AS1 in RT4
468 and T24 cells(Fig. 5h). Taken together, these results indicate that TMPO-
469 AS1 upregulates E2F1 protein levels via OTUB1-mediated
470 deubiquitination and the consequent protein stabilization.

471

472 **E2F1 promotes cell proliferation, migration, and invasion**
473 **of BC cells, and inhibits cell apoptosis *in vitro***

474 E2F1 is associated with cell proliferation, cell cycle progression,
475 apoptosis, cancer metastasis, and invasiveness [48]. Hence, we speculated
476 that E2F1 would promote BC tumorigenesis and development. According
477 to the data retrieved from TCGA and the GEO (GSE133624) databases,
478 the expression of E2F1 was remarkably higher in BC tissues than that in
479 normal tissues (Fig. 6a,b). Furthermore, western blotting and IHC
480 analyses showed that the expression of E2F1 was upregulated in six
481 paired BC tissues compared with the adjacent normal tissues (Fig. 6c,d).
482 As anticipated, further function experiments demonstrated that E2F1
483 knockdown significantly inhibited cell proliferation (Fig. 6e, f),
484 migration(Fig. 6g), invasion (Fig. 6h) , and induced apoptosis (Fig. 6i),
485 whereas the overexpression of E2F1 led to the opposite effects.
486 Altogether, these results reveal that E2F1 promotes malignant phenotypes
487 of BC cells.

488 **TMPO-AS1 regulates malignant phenotypes of BC via E2F1 *in***
489 ***vitro***

490 Since overexpression of either E2F1 or TMPO-AS1 enhanced the
491 proliferation, migration, and invasion of BC cells, and TMPO-AS1
492 upregulated E2F1 protein levels, we hypothesized that TMPO-AS1 would
493 promote BC progression via E2F1. To prove this theory, we restored
494 E2F1 expression in TMPO-AS1-silenced BC cells (Fig. 7a) and
495 performed MTT, colony formation, wound healing , and transwell assays
496 As shown, E2F1 restoration in BC cells significantly reversed the
497 inhibition on cell proliferation (Fig. 7b, c), migration (Fig. 7d) and
498 invasion (Fig. 7e) induced by silencing TMPO-AS1. Furthermore,
499 TMPO-AS1 silencing-mediated promotion of apoptosis could be
500 abrogated by E2F1 overexpression (Fig. 7f). Therefore, our data
501 demonstrate that TMPO-AS1 promotes BC cell proliferation, migration,
502 invasion, and survival via E2F1 *in vitro*.

503

504 **TMPO-AS1 regulates BC growth via E2F1 *in vivo***

505 To investigate whether TMPO-AS1 would promote BC growth via
506 E2F1 *in vivo*, we performed xenograft experiments. RT4 cells with the
507 negative control, stably knockdown of TMPO-AS1, or co-treatment of
508 TMPO-AS1 depletion and E2F1 were subcutaneously injected into the

509 flanks of nude mice, respectively. Every 5 days, the tumor volumes were
510 measured. Results showed that TMPO-AS1 knockout significantly
511 suppressed tumor growth compared to the control group, whereas E2F1
512 overexpression abolished the inhibitory effect on tumor growth induced
513 by TMPO-AS1 knockout (Fig. 8a,b). Furthermore, IHC staining showed
514 that TMPO-AS1 depletion led to a substantial decrease of Ki-67 and
515 E2F1 protein levels, and to a notable increase in the expression of
516 caspase-3. Of note, this phenotype was reversed by the overexpression of
517 E2F1 (Fig. 8c). Collectively, the above findings demonstrate that TMPO-
518 AS1 regulates tumor growth of BC via E2F1 *in vivo*.

519

520 **Discussion**

521 Bladder cancer is the most common urinary system malignancy,
522 causing heavy burden worldwide. Therefore, it is imperative to elucidate
523 the carcinogenesis of BC. In our study, we show that E2F1 stimulates
524 TMPO-AS1 transcription. In turn, TMPO-AS1 facilitates the interaction
525 of E2F1 with OTUB1, thereby upregulates E2F1 protein levels.

526 Altogether, our study highlights TMPO-AS1 forms a positive feedback
527 loop with E2F1 in BC, and suggests that both TMPO-AS1 and E2F1 are
528 potential therapeutic targets for BC patients.

529 An increasing number of studies have demonstrated lncRNAs play a
530 role in tumor initiation, development, and progression in numerous
531 cancers, including BC [13, 16, 49]. Here, we found that TMPO-AS1 is
532 highly expressed in BC, and correlates with poor prognoses. We
533 performed *in vitro* experiment and proved that TMPO-AS1 could
534 function as an oncogene, consistent with previous studies [17, 50, 51, 52].
535 Our studies suggests TMPO-AS1 may be a potential therapeutic target in
536 BC patients.

537 lncRNAs are regulated by multiple transcription factors. E2F1 is a
538 potent transcription factor, already demonstrated to regulate the
539 expression of lncRNAs [47, 51, 53]. Thousands of abnormally expressed
540 lncRNAs have been reported in BC [14]. However, little is known about
541 the upstream regulation of these lncRNAs. For instance, how E2F1
542 regulates the expression of lncRNAs is yet to be fully understood. In the
543 present study, we found that TMPO-AS1 positively correlates with E2F1
544 and that E2F1 activates the transcription of TMPO-AS1. Therefore, our
545 data, showing that TMPO-AS1 is upregulated in BC due to E2F1,
546 contribute to a better understanding of the regulatory mechanisms
547 upstream of lncRNAs.

548 The function of a lncRNA depends largely on its subcellular location.

549 LncRNAs enriched in nucleus are involved in transcriptional regulation,
550 chromosomal interactions, and RNA processing, while cytoplasmic-
551 enriched lncRNAs participate in the post-transcriptional and translational
552 regulation [54]. In the present study, TMPO-AS1 was identified to be
553 enriched in both the nucleus and cytoplasm of BC cells based on FISH
554 assay. Of note, we found TMPO-AS1 directly binds to E2F1, increasing
555 its stability. The knockdown of TMPO-AS1 resulted in higher E2F1
556 ubiquitination levels. In the current study, we reveal that TMPO-AS1
557 facilitates the interaction of E2F1 with OTUB1, a deubiquitinase, and
558 therefore is indirectly responsible for the deubiquitination-mediated
559 increase in E2F1 protein stability. While the specific ubiquitinating
560 linkage of E2F1 by OTUB1 is of interest that should be identified in
561 future investigation. Numerous studies have revealed that TMPO-AS1
562 contributes to tumorigenesis. However, most of them suggest that this is
563 mediated *via* a TMPO-AS1-miRNA-mRNA axis [17, 18, 51, 52], while
564 others propose that TMPO-AS1 forms RNA-RNA complexes to regulate
565 gene expression [19, 55]. Very recently, a study has shown that TMPO-
566 AS1 promotes BC cell growth via a TMPO-AS1/miR-98-5p/EBF1
567 positive feedback loop [51]. However, this study only elucidated the
568 function of TMPO-AS1 as a miRNA “sponge” for *EBF1* mRNA and only
569 *in vitro*; the role of TMPO-AS1 in BC, *in vivo*, is still unknown. Our

570 study provide the first evidence that TMPO-AS1 could interaction with
571 proteins, and thereby influences protein-protein interactions, revealing a
572 novel regulatory pattern of TMPO-AS1.

573 Transcription factor E2F1 has been reported to play a vital role in
574 cancer stemness, progression, and chemoresistance [46, 56, 57]. It is well
575 known that E2F1 is overexpressed in several cancers, and upregulated
576 E2F1 is a strong predictor of BC progression, from the superficial to the
577 invasive [48]. FOXD2-AS1 was reported to promote BC progression and
578 recurrence via the activation of the Akt/E2F1 signaling pathway [16]. In
579 our study, we found that the overexpression of either E2F1 or TMPO-
580 AS1 boosted cell proliferation, migration, invasion, and inhibits the
581 apoptosis of BC cells; their knockdown obviously led to the opposite.
582 However, up to now, it was not clear whether TMPO-AS1 could function
583 as an oncogene in an E2F1-mediated manner. Importantly, function
584 recovery assays *in vitro* and rescue experiments *in vivo* indeed showed
585 that TMPO-AS1 promotes BC growth in an E2F1-dependent manner.
586 Our results, along with previous studies, demonstrate that E2F1 promotes
587 cancer carcinogenesis, development, and progression. Several studies
588 indicated that positive feedback loops are extremely important for the
589 regulation of cancer carcinogenesis and progression [16, 51, 58]. Here,
590 we disclose a new positive feedback loop that contributes to BC

591 tumorigenesis, involving TMPO-AS1 and E2F1. Altogether, our data
592 support a mutual regulatory pattern between lncRNAs and transcription
593 factors, which may lead to increased oncogenic activity in cancer
594 development.

595 Despite we indeed reveal novel mechanisms for BC carcinogenesis, it
596 is undeniable that our work has limitations as follows: our study lacks of
597 sufficient clinical BC samples, thus we validate the clinical significance
598 of TMPO-AS1 using online software rather than our own data. In
599 addition, the specific sequence and structure of TMPO-AS1 contributing
600 to OTUB1-mediated E2F1 deubiquitination remain unknown. And the
601 downstream oncogenic molecules of E2F1 in BC are still unclear. We
602 will investigate those unknown but interesting questions in future study.

603 In summary, our study propose a novel mechanism of tumorigenesis
604 in BC: TMPO-AS1 exerts oncogenic functions in an E2F1-dependent
605 manner. Therefore, the TMPO-AS1/E2F1 should be considered in the
606 development of new therapeutic approaches for BC.

607

608 **Conclusions**

609 Collectively, our study uncovered the upstream and downstream
610 regulation of TMPO-AS1, revealing a novel mechanism of BC
611 tumorigenesis, development and progression. The TMPO-AS1/E2F1

612 positive feedback loop may be a potential new target for the treatment of
613 BC patients.

614

615 **List of abbreviations**

616 BC: bladder cancer

617 lncRNAs: long non-coding RNAs

618 TMPO-AS1:TMPO antisense RNA 1

619 E2F1: E2F transcription factor 1

620 OTUB1: OTU domain-containing ubiquitin aldehyde binding 1

621 NMIBC: non-muscle-invasive bladder cancer

622 MIBC: muscle-invasive bladder cancer

623 miRNA: microRNA

624 TF: transcription factor

625 TCGA: The Cancer Genome Atlas

626 ChIP: Chromatin immunoprecipitation

627 FISH: Fluorescence in situ hybridization

628 IHC: Immunohistochemistry

629 qRT-PCR: quantitative Real-time polymerase chain reaction

630 RIP: RNA immunoprecipitation

631 Co-IP: Co-immunoprecipitation

632

633 **Declarations**

634 **Ethics approval and consent to participate**

635 This study was approved by the Ethics Committee of The Third
636 Xiangya Hospital, and written informed consent was obtained from each
637 patient involved in the study.

638

639 **Consent for publication**

640 Written informed consent for publication was obtained from all
641 participants involved in our study.

642

643 **Availability of data and materials**

644 The datasets used and analyzed in the current study are available from
645 the corresponding author on reasonable request.

646

647 **Competing interests**

648 The authors declare that they have no conflict of interest.

649

650 **Funding**

651 This work was financially supported by the National Natural Science
652 Foundation of China (81874137), the Outstanding Youth Foundation of
653 Hunan Province (2018JJ1047), the Huxiang Young Talent Project
654 (2016RS3022), the Hunan Province Science and Technology Talent
655 Promotion Project (2019TJ-Q10), and the Independent Exploration and
656 Innovation Project of Central South University, Grant/Award Number:
657 2019zzts825.

658

659 **Authors' contributions**

660 KC and YY Z designed this study. JY L and MQ X collected the
661 clinical samples. JY L and YY Z contributed to the experiments
662 implementation. YX C, DH, and LX analyzed the data. KC, YY Z, and
663 YX Zhu drafted the manuscript. LG, ZW W, and LP D edited the
664 manuscript. All authors read and approved the final manuscript.

665

666 **Acknowledgements**

667 Not applicable.

668

669 **Authors' information**

670 **Affiliations**

671 **Department of Oncology, the Third Xiangya Hospital of Central**
672 **South University, Changsha 410013, China.**

673 Yeyu Zhang, Yuxing Zhu, Mengqing Xiao, Yaxin Cheng, Liang Xiang,
674 Lian Gong, Zhanwang Wang, Liping Deng, and Ke Cao

675

676 **Department of Respiratory, The Second People's Hospital of Hunan**
677 **Province, Changsha 410007, China.**

678 Dong He

679

680 **Department of Urology, the Third Xiangya Hospital of Central South**
681 **University, Changsha 410013**

682 Jianye Liu

683

684 **Corresponding author**

685 Correspondence to Ke Cao.

686

687 **Reference**

- 688 1. Antoni S, Ferlay J, Soerjomataram I, Znaor A, Jemal A, Bray F. Bladder Cancer
689 Incidence and Mortality: A Global Overview and Recent Trends. Eur Urol.
690 2017;71:96-108.

- 691 2. Bray F, Ferlay J, Soerjomataram I, Siegel RL, Torre LA, Jemal A. Global cancer
692 statistics 2018: GLOBOCAN estimates of incidence and mortality worldwide for 36
693 cancers in 185 countries. *CA Cancer J Clin.* 2018;68:394-424.
- 694 3. Robertson AG, Kim J, Al-Ahmadie H, Bellmunt J, Guo G, Cherniack AD, et al.
695 Comprehensive Molecular Characterization of Muscle-Invasive Bladder Cancer. *Cell.*
696 2018;174:1033.
- 697 4. Berdik C. Unlocking bladder cancer. *Nature.* 2017;551:S34-S5.
- 698 5. Ponting CP, Oliver PL, Reik W. Evolution and functions of long noncoding RNAs.
699 *Cell.* 2009;136:629-41.
- 700 6. Adams BD, Parsons C, Walker L, Zhang WC, Slack FJ. Targeting noncoding
701 RNAs in disease. *J Clin Invest.* 2017;127:761-71.
- 702 7. Mercer TR, Dinger ME, Mattick JS. Long non-coding RNAs: insights into
703 functions. *Nat Rev Genet.* 2009;10:155-9.
- 704 8. Tang J, Yan T, Bao Y, Shen C, Yu C, Zhu X, et al. LncRNA GLCC1 promotes
705 colorectal carcinogenesis and glucose metabolism by stabilizing c-Myc. *Nat*
706 *Commun.* 2019;10:3499.
- 707 9. Gupta RA, Shah N, Wang KC, Kim J, Horlings HM, Wong DJ, et al. Long non-
708 coding RNA HOTAIR reprograms chromatin state to promote cancer metastasis.
709 *Nature.* 2010;464:1071-6.

710 10. Tsai MC, Manor O, Wan Y, Mosammaparast N, Wang JK, Lan F, et al. Long
711 noncoding RNA as modular scaffold of histone modification complexes. *Science*.
712 2010;329:689-93.

713 11. Wang CJ, Zhu CC, Xu J, Wang M, Zhao WY, Liu Q, et al. The lncRNA UCA1
714 promotes proliferation, migration, immune escape and inhibits apoptosis in gastric
715 cancer by sponging anti-tumor miRNAs. *Mol Cancer*. 2019;18:115.

716 12. Liu Z, Xie D, Zhang H. Long noncoding RNA neuroblastoma-associated
717 transcript 1 gene inhibits malignant cellular phenotypes of bladder cancer through
718 miR-21/SOCS6 axis. *Cell Death Dis*. 2018;9:1042.

719 13. Zhan Y, Chen Z, Li Y, He A, He S, Gong Y, et al. Long non-coding RNA
720 DANCR promotes malignant phenotypes of bladder cancer cells by modulating the
721 miR-149/MSI2 axis as a ceRNA. *J Exp Clin Cancer Res*. 2018;37:273.

722 14. Martens-Uzunova ES, Bottcher R, Croce CM, Jenster G, Visakorpi T, Calin GA.
723 Long noncoding RNA in prostate, bladder, and kidney cancer. *Eur Urol*.
724 2014;65:1140-51.

725 15. Fan Y, Shen B, Tan M, Mu X, Qin Y, Zhang F, et al. TGF-beta-induced
726 upregulation of malat1 promotes bladder cancer metastasis by associating with suz12.
727 *Clin Cancer Res*. 2014;20:1531-41.

728 16. Su F, He W, Chen C, Liu M, Liu H, Xue F, et al. The long non-coding RNA
729 FOXD2-AS1 promotes bladder cancer progression and recurrence through a positive
730 feedback loop with Akt and E2F1. *Cell Death Dis*. 2018;9:233.

731 17. Guo X, Wang Y. LncRNA TMPO-AS1 promotes hepatocellular carcinoma cell
732 proliferation, migration and invasion through sponging miR-329-3p to stimulate
733 FOXK1-mediated AKT/mTOR signaling pathway. *Cancer Med.* 2020;9:5235-46.

734 18. Li Z, Feng Y, Zhang Z, Cao X, Lu X. TMPO-AS1 promotes cell proliferation of
735 thyroid cancer via sponging miR-498 to modulate TMPO. *Cancer Cell Int.*
736 2020;20:294.

737 19. Mitobe Y, Ikeda K, Suzuki T, Takagi K, Kawabata H, Horie-Inoue K, et al.
738 ESR1-Stabilizing Long Noncoding RNA TMPO-AS1 Promotes Hormone-Refractory
739 Breast Cancer Progression. *Mol Cell Biol.* 2019;39.

740 20. Peng F, Wang R, Zhang Y, Zhao Z, Zhou W, Chang Z, et al. Differential
741 expression analysis at the individual level reveals a lncRNA prognostic signature for
742 lung adenocarcinoma. *Mol Cancer.* 2017;16:98.

743 21. Huarte M, Guttman M, Feldser D, Garber M, Koziol MJ, Kenzelmann-Broz D, et
744 al. A large intergenic noncoding RNA induced by p53 mediates global gene
745 repression in the p53 response. *Cell.* 2010;142:409-19.

746 22. Tsantoulis PK, Gorgoulis VG. Involvement of E2F transcription factor family in
747 cancer. *Eur J Cancer.* 2005;41:2403-14.

748 23. Feldstein O, Nizri T, Doniger T, Jacob J, Rechavi G, Ginsberg D. The long non-
749 coding RNA ERIC is regulated by E2F and modulates the cellular response to DNA
750 damage. *Mol Cancer.* 2013;12:131.

751 24. Lee SR, Roh YG, Kim SK, Lee JS, Seol SY, Lee HH, et al. Activation of EZH2
752 and SUZ12 Regulated by E2F1 Predicts the Disease Progression and Aggressive
753 Characteristics of Bladder Cancer. *Clin Cancer Res.* 2015;21:5391-403.

754 25. Mofers A, Pellegrini P, Linder S, D'Arcy P. Proteasome-associated
755 deubiquitinases and cancer. *Cancer Metastasis Rev.* 2017;36:635-53.

756 26. Campanero MR, Flemington EK. Regulation of E2F through ubiquitin-
757 proteasome-dependent degradation: stabilization by the pRB tumor suppressor
758 protein. *Proc Natl Acad Sci U S A.* 1997;94:2221-6.

759 27. Wang B, Ma A, Zhang L, Jin WL, Qian Y, Xu G, et al. POH1 deubiquitylates and
760 stabilizes E2F1 to promote tumour formation. *Nat Commun.* 2015;6:8704.

761 28. Xia M, Liu CJ, Zhang Q, Guo AY. GEDS: A Gene Expression Display Server for
762 mRNAs, miRNAs and Proteins. *Cells.* 2019;8.

763 29. Li J, Han L, Roebuck P, Diao L, Liu L, Yuan Y, et al. TANRIC: An Interactive
764 Open Platform to Explore the Function of lncRNAs in Cancer. *Cancer Res.*
765 2015;75:3728-37.

766 30. Chen X, Li A, Sun BF, Yang Y, Han YN, Yuan X, et al. 5-methylcytosine
767 promotes pathogenesis of bladder cancer through stabilizing mRNAs. *Nat Cell Biol.*
768 2019;21:978-90.

769 31. Tang Z, Li C, Kang B, Gao G, Li C, Zhang Z. GEPIA: a web server for cancer
770 and normal gene expression profiling and interactive analyses. *Nucleic Acids Res.*
771 2017;45:W98-W102.

772 32. Zhang Q, Liu W, Zhang HM, Xie GY, Miao YR, Xia M, et al. hTFtarget: A
773 Comprehensive Database for Regulations of Human Transcription Factors and Their
774 Targets. *Genomics Proteomics Bioinformatics*. 2020.

775 33. Zhou KR, Liu S, Sun WJ, Zheng LL, Zhou H, Yang JH, et al. ChIPBase v2.0:
776 decoding transcriptional regulatory networks of non-coding RNAs and protein-coding
777 genes from ChIP-seq data. *Nucleic Acids Res*. 2017;45:D43-D50.

778 34. Khan A, Fornes O, Stigliani A, Gheorghe M, Castro-Mondragon JA, van der Lee
779 R, et al. JASPAR 2018: update of the open-access database of transcription factor
780 binding profiles and its web framework. *Nucleic Acids Res*. 2018;46:D260-D6.

781 35. Zhao Z, Bai J, Wu A, Wang Y, Zhang J, Wang Z, et al. Co-LncRNA:
782 investigating the lncRNA combinatorial effects in GO annotations and KEGG
783 pathways based on human RNA-Seq data. *Database (Oxford)*. 2015;2015.

784 36. Zhou Y, Zhou B, Pache L, Chang M, Khodabakhshi AH, Tanaseichuk O, et al.
785 Metascape provides a biologist-oriented resource for the analysis of systems-level
786 datasets. *Nat Commun*. 2019;10:1523.

787 37. Agostini F, Zanzoni A, Klus P, Marchese D, Cirillo D, Tartaglia GG. catRAPID
788 omics: a web server for large-scale prediction of protein-RNA interactions.
789 *Bioinformatics*. 2013;29:2928-30.

790 38. Tuvshinjargal N, Lee W, Park B, Han K. PRIdictor: Protein-RNA Interaction
791 predictor. *Biosystems*. 2016;139:17-22.

792 39. Yan Y, Zhang D, Zhou P, Li B, Huang SY. HDOCK: a web server for protein-
793 protein and protein-DNA/RNA docking based on a hybrid strategy. *Nucleic Acids*
794 *Res.* 2017;45:W365-W73.

795 40. Radivojac P, Vacic V, Haynes C, Cocklin RR, Mohan A, Heyen JW, et al.
796 Identification, analysis, and prediction of protein ubiquitination sites. *Proteins.*
797 2010;78:365-80.

798 41. Zeng Q, Liu J, Cao P, Li J, Liu X, Fan X, et al. Inhibition of REDD1 Sensitizes
799 Bladder Urothelial Carcinoma to Paclitaxel by Inhibiting Autophagy. *Clin Cancer*
800 *Res.* 2018;24:445-59.

801 42. Zhu Y, He D, Bo H, Liu Z, Xiao M, Xiang L, et al. The MRVI1-AS1/ATF3
802 signaling loop sensitizes nasopharyngeal cancer cells to paclitaxel by regulating the
803 Hippo-TAZ pathway. *Oncogene.* 2019;38:6065-81.

804 43. Liu JY, Zeng QH, Cao PG, Xie D, Yang F, He LY, et al. SPAG5 promotes
805 proliferation and suppresses apoptosis in bladder urothelial carcinoma by upregulating
806 Wnt3 via activating the AKT/mTOR pathway and predicts poorer survival.
807 *Oncogene.* 2018;37:3937-52.

808 44. Postepska-Igielska A, Giwojna A, Gasri-Plotnitsky L, Schmitt N, Dold A,
809 Ginsberg D, et al. LncRNA Khps1 Regulates Expression of the Proto-oncogene
810 SPHK1 via Triplex-Mediated Changes in Chromatin Structure. *Mol Cell.*
811 2015;60:626-36.

812 45. Parise P, Finocchiaro G, Masciadri B, Quarto M, Francois S, Mancuso F, et al.
813 Lap2alpha expression is controlled by E2F and deregulated in various human tumors.
814 Cell Cycle. 2006;5:1331-41.

815 46. Logotheti S, Marquardt S, Gupta SK, Richter C, Edelhauser BAH, Engelmann D,
816 et al. LncRNA-SLC16A1-AS1 induces metabolic reprogramming during Bladder
817 Cancer progression as target and co-activator of E2F1. Theranostics. 2020;10:9620-
818 43.

819 47. Yu L, Fang F, Lu S, Li X, Yang Y, Wang Z. lncRNA-HIT promotes cell
820 proliferation of non-small cell lung cancer by association with E2F1. Cancer Gene
821 Ther. 2017;24:221-6.

822 48. Lee JS, Leem SH, Lee SY, Kim SC, Park ES, Kim SB, et al. Expression signature
823 of E2F1 and its associated genes predict superficial to invasive progression of bladder
824 tumors. J Clin Oncol. 2010;28:2660-7.

825 49. Zhang Y, Tang B, Song J, Yu S, Li Y, Su H, et al. Lnc-PDZD7 contributes to
826 stemness properties and chemosensitivity in hepatocellular carcinoma through EZH2-
827 mediated ATOH8 transcriptional repression. J Exp Clin Cancer Res. 2019;38:92.

828 50. Huang W, Su X, Yan W, Kong Z, Wang D, Huang Y, et al. Overexpression of
829 AR-regulated lncRNA TMPO-AS1 correlates with tumor progression and poor
830 prognosis in prostate cancer. Prostate. 2018;78:1248-61.

831 51. Luo H, Yang L, Liu C, Wang X, Dong Q, Liu L, et al. TMPO-AS1/miR-98-
832 5p/EBF1 feedback loop contributes to the progression of bladder cancer. *Int J*
833 *Biochem Cell Biol.* 2020;122:105702.

834 52. Cui H, Zhao J. LncRNA TMPO-AS1 serves as a ceRNA to promote osteosarcoma
835 tumorigenesis by regulating miR-199a-5p/WNT7B axis. *J Cell Biochem.*
836 2020;121:2284-93.

837 53. Berteaux N, Lottin S, Monte D, Pinte S, Quatannens B, Coll J, et al. H19 mRNA-
838 like noncoding RNA promotes breast cancer cell proliferation through positive
839 control by E2F1. *J Biol Chem.* 2005;280:29625-36.

840 54. Schmitt AM, Chang HY. Long Noncoding RNAs in Cancer Pathways. *Cancer*
841 *Cell.* 2016;29:452-63.

842 55. Qin Z, Zheng X, Fang Y. Long noncoding RNA TMPO-AS1 promotes
843 progression of non-small cell lung cancer through regulating its natural antisense
844 transcript TMPO. *Biochem Biophys Res Commun.* 2019;516:486-93.

845 56. Lu G, Li Y, Ma Y, Lu J, Chen Y, Jiang Q, et al. Long noncoding RNA
846 LINC00511 contributes to breast cancer tumourigenesis and stemness by inducing the
847 miR-185-3p/E2F1/Nanog axis. *J Exp Clin Cancer Res.* 2018;37:289.

848 57. Fang Z, Gong C, Yu S, Zhou W, Hassan W, Li H, et al. NFYB-induced high
849 expression of E2F1 contributes to oxaliplatin resistance in colorectal cancer via the
850 enhancement of CHK1 signaling. *Cancer Lett.* 2018;415:58-72.

851 58. Xu MD, Wang Y, Weng W, Wei P, Qi P, Zhang Q, et al. A Positive Feedback
852 Loop of lncRNA-PVT1 and FOXM1 Facilitates Gastric Cancer Growth and Invasion.
853 Clin Cancer Res. 2017;23:2071-80.

854

855 **Figure legends**

856 **Figure 1. The upregulation of TMPO-AS1 predicts the poor**
857 **prognosis of BC patients. a** TMPO-AS1 is highly expressed in the
858 majority of cancers according to GEDS. **b, c** The expression of TMPO-
859 AS1 in BC *versus* normal tissues was verified by analyzing TCGA and
860 TANRIC data. **d** qRT-PCR was conducted to validate TMPO-AS1
861 expression in six pairs of BC tissues and adjacent normal tissues collected
862 in this study(replicate=3). **e-g** The expression profile of TMPO-AS1 in
863 BC, as per two datasets retrieved for the GEO: GSE133624 and
864 GSE120736. **h** The disease-free survival curve showed high levels of
865 TMPO-AS1 expression were associated with poor prognosis of BC
866 patients using GEPIA. * $P < 0.05$, ** $P < 0.01$, *** $P < 0.001$.

867

868 **Figure 2. TMPO-AS1 promotes cell proliferation, migration, and**
869 **invasion, and the survival of BC cells *in vitro*. a** qRT-PCR showing the
870 mRNA levels of TMPO-AS1 in five bladder cell lines (BIU87, 5637,
871 T24, EJ, and RT4). **b** The efficiencies of TMPO-AS1 knockdown or

872 overexpression in RT4 and T24 cells were examined by qRT-PCR.
873 Mock, the negative control; Si-TMPO-AS1, siRNA targeting TMPO-
874 AS1; OE-TMPO-AS1, ectopic expression of TMPO-AS1. **c, d** The effect
875 of TMPO-AS1 knockdown and overexpression on cell proliferation was
876 measured using MTT and colony formation assays. **e, f** The effects of
877 TMPO-AS1 knockdown or overexpression on RT4 and T24 cells'
878 migration and invasion were evaluated via wound healing and transwell
879 assays. **g** Cell apoptosis was analyzed by flow cytometry in RT4 and T24
880 cells silencing or overexpressing TMPO-AS1, stained with Annexin V-
881 PE/7-AAD. Error bars represent the mean \pm S.D. from three independent
882 experiments. * $P < 0.05$, ** $P < 0.01$, *** $P < 0.001$ versus Mock group
883 (negative control).

884

885 **Figure 3. E2F1 binds to TMPO-AS1 promoter and activates its**
886 **transcription. a** The potential transcription factors of TMPO-AS1 were
887 predicted using ChIPBase v2.0 and hTFtarget. **b** The pathway enrichment
888 analysis of genes co-expressed with TMPO-AS1 using Metascape. **c, d**
889 The correlation between TMPO-AS1 and E2F1 mRNA expression in BC
890 tissues was assessed using the Pearson's correlation analysis in datasets
891 retrieved from TCGA and the GEO (GSE133624). **e** The expression of
892 TMPO-AS1 was evaluated using qRT-PCR in RT4 and T24 cells

893 silencing or overexpressing E2F1. Mock, the negative control; Si-E2F1,
894 siRNA targeting E2F1; OE-E2F1, ectopic expression of E2F1. **f** The
895 binding sites between E2F1 and TMPO-AS1 promoter region were
896 predicted using JASPAR. **g** Luciferase reporter assays were conducted to
897 measure the luciferase activity of TMPO-AS1 promoter in RT4 and T24
898 cells overexpressing E2F1. Vector, the negative control. **h** ChIP assay
899 demonstrated E2F1 bound to the TMPO-AS1 promoter. Error bars
900 represent the mean \pm S.D. from three independent experiments. * $P <$
901 0.05, ** $P < 0.01$ *versus* negative controls.

902

903 **Figure 4. TMPO-AS1 upregulates E2F1 protein levels via the**
904 **promotion of protein stability.** **a** The interaction between TMPO-AS1
905 and E2F1 was predicted using catRAPID. **b** RNA pull-down assay was
906 performed to validate the potential interaction between TMPO-AS1 and
907 E2F1 in RT4 and T24 cells overexpressing TMPO-AS1. **c** RIP assay was
908 performed to further confirm the interaction between E2F1 and TMPO-
909 AS1, in TMPO-AS1 overexpressing RT4 and T24 cells; IgG was used as
910 a RIP negative control. Error bars represent the mean \pm S.D. from three
911 independent experiments. *** $P < 0.001$ *versus* negative control. **d** *E2F1*
912 mRNA expression was assessed using qRT-PCR in TMPO-AS1 silencing
913 or overexpressing BC cells. **e** E2F1 protein expression was evaluated via

914 western blotting in TMPO-AS1 silencing or overexpressing RT4 and T24
915 cells. **f** Western blotting showing proteasome inhibitor MG132 protein
916 increased E2F1 stability in cycloheximide-treated RT4 and T24 cells.
917 CHX, cycloheximide. **g** Western blotting showing decreased E2F1
918 stability was observed in TMPO-AS1 knockdown RT4 and T24 cells.

919

920 **Figure 5. TMPO-AS1 stabilizes E2F1 via OTUB1-mediated**
921 **deubiquitination**

922 **a** TMPO-AS1 cellular localization was evaluated using FISH. **b** RNA
923 pull-down assays demonstrated that OTUB1 was the most likely
924 deubiquitinase binding to TMPO-AS among a group of deubiquitinases
925 (OTUB1, UCHL5, USP5, COPS6, and PSMD14). **c** RIP assays were
926 performed to validate the interaction between TMPO-AS1 and OTUB1,
927 in the context of TMPO-AS1 overexpressing RT4 and T24 cells; IgG was
928 used as a RIP negative control. Error bars represent the mean \pm S.D. from
929 three independent experiments. $***P < 0.001$ versus negative control. **d**
930 Western blotting showing TMPO-AS1 silencing had no effect on OTUB1
931 protein levels in RT4 and T24 cells. **e** Western blotting showing
932 knockdown of OTUB1 decreased E2F1 protein levels in RT4 and T24
933 cells. Si- OTUB1, siRNA targeting OTUB1. **f** HDCK showing
934 E2F1(yellow) and OTUB1(brown) were very likely to bind to each other.

935 **g** Co-IP assays were performed in control or si-TMPO-AS1 treated RT4
936 and T24 cells using an anti-E2F1 antibody, followed by western blotting
937 to analyze the ubiquitin levels of E2F1. **h** RT4 and T24 cells transfected
938 with the empty vector, TMPO-AS1 overexpressing, or along with si-
939 OTUB1 were subjected to immunoprecipitation with anti-E2F1 antibody,
940 followed by western blotting with an anti-ubiquitin antibody.

941

942 **Figure 6. E2F1 promotes the proliferation, migration, and invasion,**

943 **and inhibits the apoptosis of BC cells *in vitro*. a, b** The transcriptional

944 expression of *E2F1* was upregulated in BC tissues compared with that in

945 normal tissues based on data retrieved from TCGA and GSE133624 . **c**

946 E2F1 protein expression was assessed via western blotting in six paired

947 BC, and adjacent normal tissue samples. **d** E2F1 protein expression was

948 also assessed using immunohistochemistry in six paired BC, and adjacent

949 normal tissue samples. **e** The MTT was performed to determine the

950 viability/proliferation of E2F1 knockdown and overexpressing RT4 and

951 T24 cells. **f** The effects of E2F1 knockdown and overexpression on BC

952 cell proliferation were assessed via colony formation assays. **g, h** The

953 migratory and invasive capacities of E2F1 knockdown and

954 overexpressing RT4 and T24 cells were evaluated via wound healing and

955 transwell assays. **i** Cell apoptosis was analyzed by flow cytometry. Error

956 bars represent the mean \pm S.D. from three independent experiments. * $P <$
957 0.05, ** $P <$ 0.01, *** $P <$ 0.001 *versus* Mock group (negative control).

958

959 **Figure 7. TMPO-AS1 promotes BC malignant phenotypes via E2F1**

960 *in vitro.* **a** TMPO-AS1 expression was evaluated using qRT-PCR in RT4
961 and T24 cells transfected with the empty vector, sh-TMPO-AS1, or co-
962 transfected with sh-TMPO-AS1 and E2F1. **b, c** MTT and colony
963 formation assays were employed to assess the proliferative ability of
964 transfected cells. **d, e** Migration and invasion were estimated using
965 wound healing and transwell assays. **f** The apoptosis in transfected BC
966 cells stained with Annexin V-PE/7-AAD was evaluated via flow
967 cytometry analysis. Error bars represent the mean \pm S.D. from three
968 independent experiments. * $P <$ 0.05, ** $P <$ 0.01, *** $P <$ 0.001.

969

970 **Figure 8. TMPO-AS1 regulates BC growth *in vivo* via E2F1.**

971 **a** Representative images of the tumor xenografts 25 days after the
972 subcutaneous injection of RT4 cells transfected with the empty vector,
973 sh-TMPO-AS1, and sh-TMPO-AS1 along with E2F1 into the flanks of
974 nude mice. **b** The tumor volumes were measured every 3 days in the three
975 groups. Three independent experiments were performed. * $P <$ 0.05. **c** The
976 expression of E2F1, Ki-67 and caspase-3 in xenografts was evaluated

977 using immunohistochemistry. Representative images are shown. **d** A
978 schematic diagram illustrating the role and mechanism of TMPO-AS1 in
979 BC tumorigenesis and progression.

980

981 **Table 1:**

982 The primer sequences used in this study.

983

984 **Additional files**

985 **Additional file 1:**

986 **Table S1.** The antibodies used in this study.

987

988 **Additional file 2:**

989 **Figure S1.** The expression of TMPO-AS1 in different clinical stages of
990 BC samples.

991

992 **Additional file 3:**

993 **Table S2.** 36 overlapping TFs, obtained from hTFtarget and ChIP Base
994 v2.0, and the correlation analysis of these TFs with TMPO-AS1.

995

996 **Additional file 4:**

997 **Table S3.** Genes that co-expressed with TMPO-AS1 retrieved from Co-
998 LncRNA.

999

1000 **Additional file 5:**

1001 **Figure S2.** E2F1 ubiquitination sites and the interactions between
1002 TMPO-AS1 and five deubiquitinases. A The potential ubiquitination sites
1003 in E2F1. B The interaction between TMPO-AS1 and five
1004 deubiquitinases(UCHL5, USP5, COPS6, PSMD14, and OTUB1)
1005 predicted by PRIdictor. C CatRAPID was used to predict the interaction
1006 pattern between TMPO-AS1 and OTUB1.

Figures

Fig.1

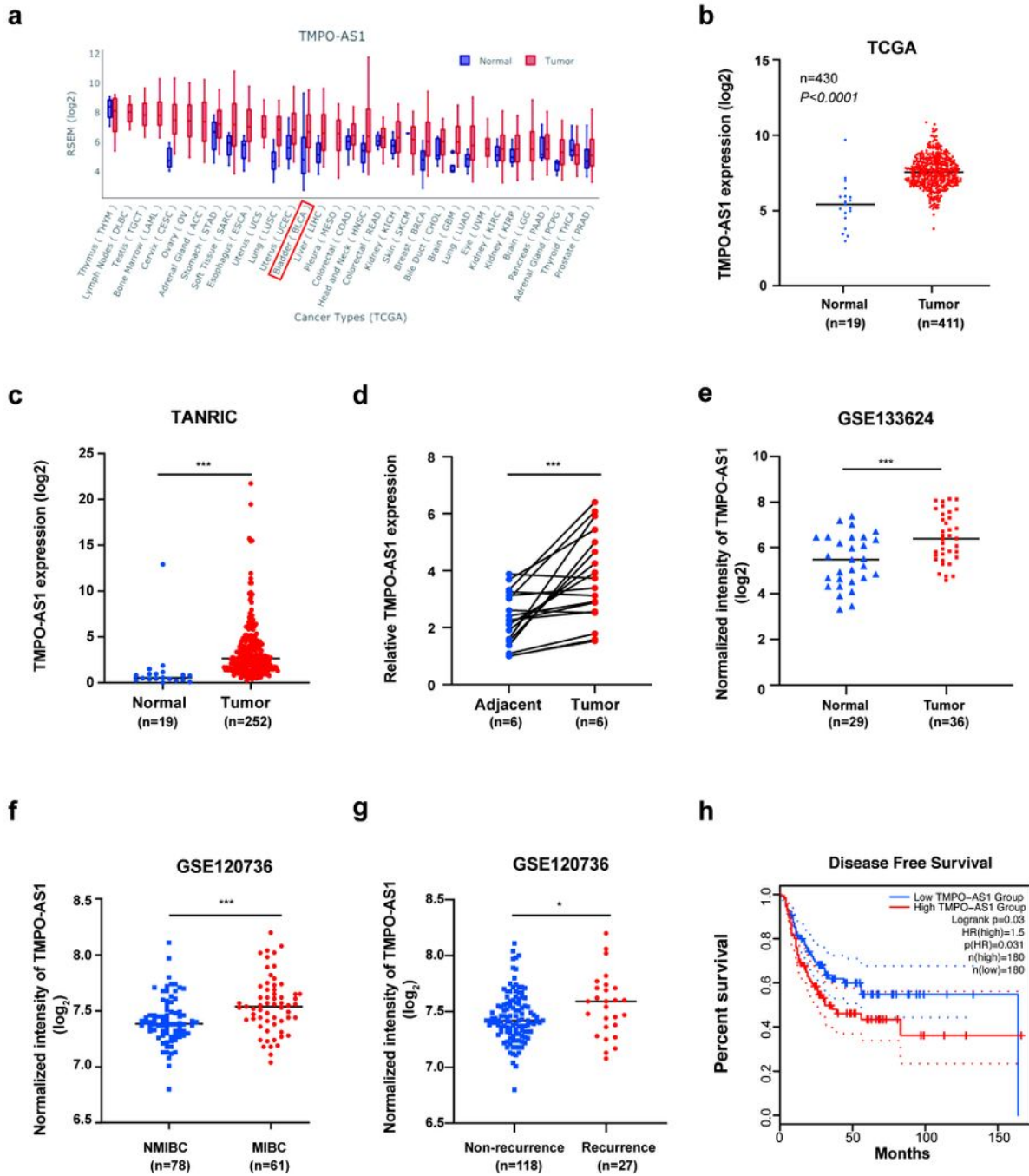


Figure 1

The upregulation of TMPO-AS1 predicts the poor prognosis of BC patients. a TMPO-AS1 is highly expressed in the majority of cancers according to GEDS. b, c The expression of TMPO-AS1 in BC versus normal tissues was verified by analyzing TCGA and TANRIC data. d qRT-PCR was conducted to validate

TMPO-AS1 expression in six pairs of BC tissues and adjacent normal tissues collected in this study (replicate=3). e-g The expression profile of TMPO-AS1 in BC, as per two datasets retrieved for the GEO: GSE133624 and GSE120736. h The disease-free survival curve showed high levels of TMPO-AS1 expression were associated with poor prognosis of BC patients using GEPIA. * P < 0.05, **P < 0.01, ***P < 0.001.

Fig.2

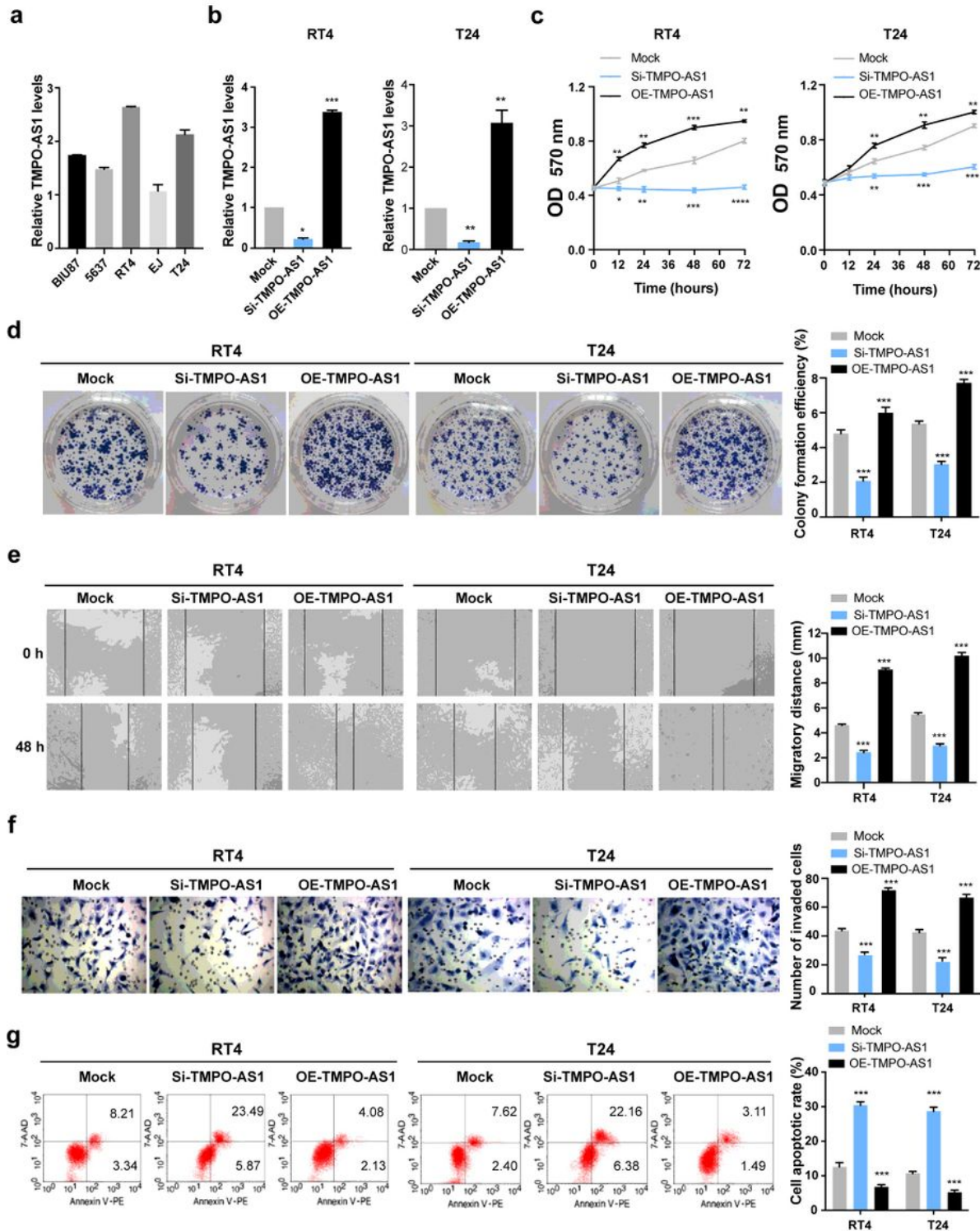
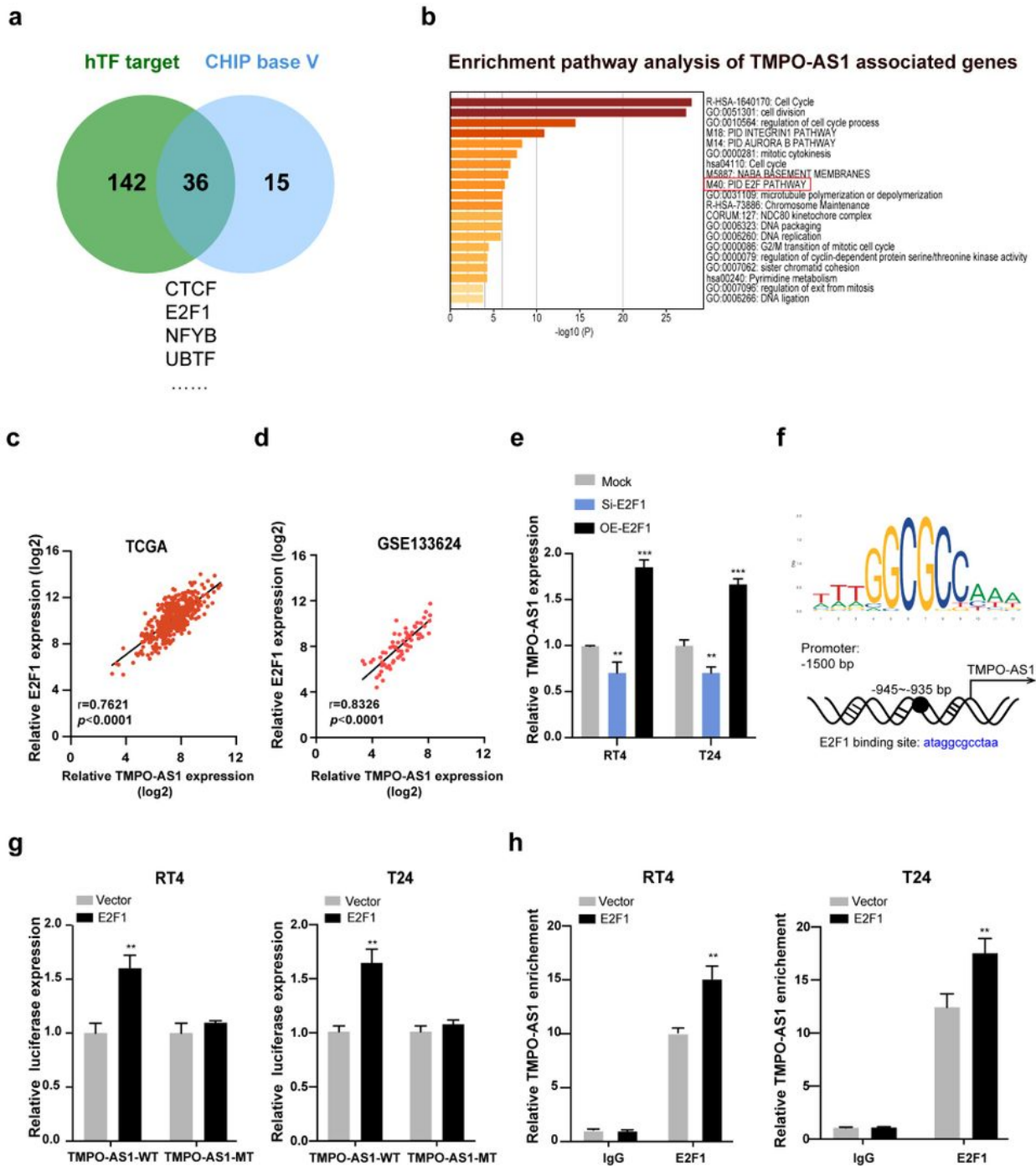


Figure 2

TMPO-AS1 promotes cell proliferation, migration, and invasion, and the survival of BC cells in vitro. a qRT-PCR showing the mRNA levels of TMPO-AS1 in five bladder cell lines (BIU87, 5637, T24, EJ, and RT4). b The efficiencies of TMPO-AS1 knockdown or overexpression in RT4 and T24 cells were examined by qRT-PCR. Mock, the negative control; Si-TMPO-AS1, siRNA targeting TMPO-AS1; OE-TMPO-AS1, ectopic expression of TMPO-AS1. c, d The effect of TMPO-AS1 knockdown and overexpression on cell proliferation was measured using MTT and colony formation assays. e, f The effects of TMPO-AS1 knockdown or overexpression on RT4 and T24 cells' migration and invasion were evaluated via wound healing and transwell assays. g Cell apoptosis was analyzed by flow cytometry in RT4 and T24 cells silencing or overexpressing TMPO-AS1, stained with Annexin V-PE/7-AAD. Error bars represent the mean \pm S.D. from three independent experiments. * $P < 0.05$, ** $P < 0.01$, *** $P < 0.001$ versus Mock group (negative control).

Fig.3**Figure 3**

E2F1 binds to TMPO-AS1 promoter and activates its transcription. a The potential transcription factors of TMPO-AS1 were predicted using ChIPBase v2.0 and hTFtarget. b The pathway enrichment analysis of genes co-expressed with TMPO-AS1 using Metascape. c, d The correlation between TMPO-AS1 and E2F1 mRNA expression in BC tissues was assessed using the Pearson's correlation analysis in datasets retrieved from TCGA and the GEO (GSE133624). e The expression of TMPO-AS1 was evaluated using

qRT-PCR in RT4 and T24 cells silencing or overexpressing E2F1. Mock, the negative control; Si-E2F1, siRNA targeting E2F1; OE-E2F1, ectopic expression of E2F1. f The binding sites between E2F1 and TMPO-AS1 promoter region were predicted using JASPAR. g Luciferase reporter assays were conducted to measure the luciferase activity of TMPO-AS1 promoter in RT4 and T24 cells overexpressing E2F1. Vector, the negative control. h ChIP assay demonstrated E2F1 bound to the TMPO-AS1 promoter. Error bars represent the mean \pm S.D. from three independent experiments. * $P < 0.05$, ** $P < 0.01$ versus negative controls.

Fig.4

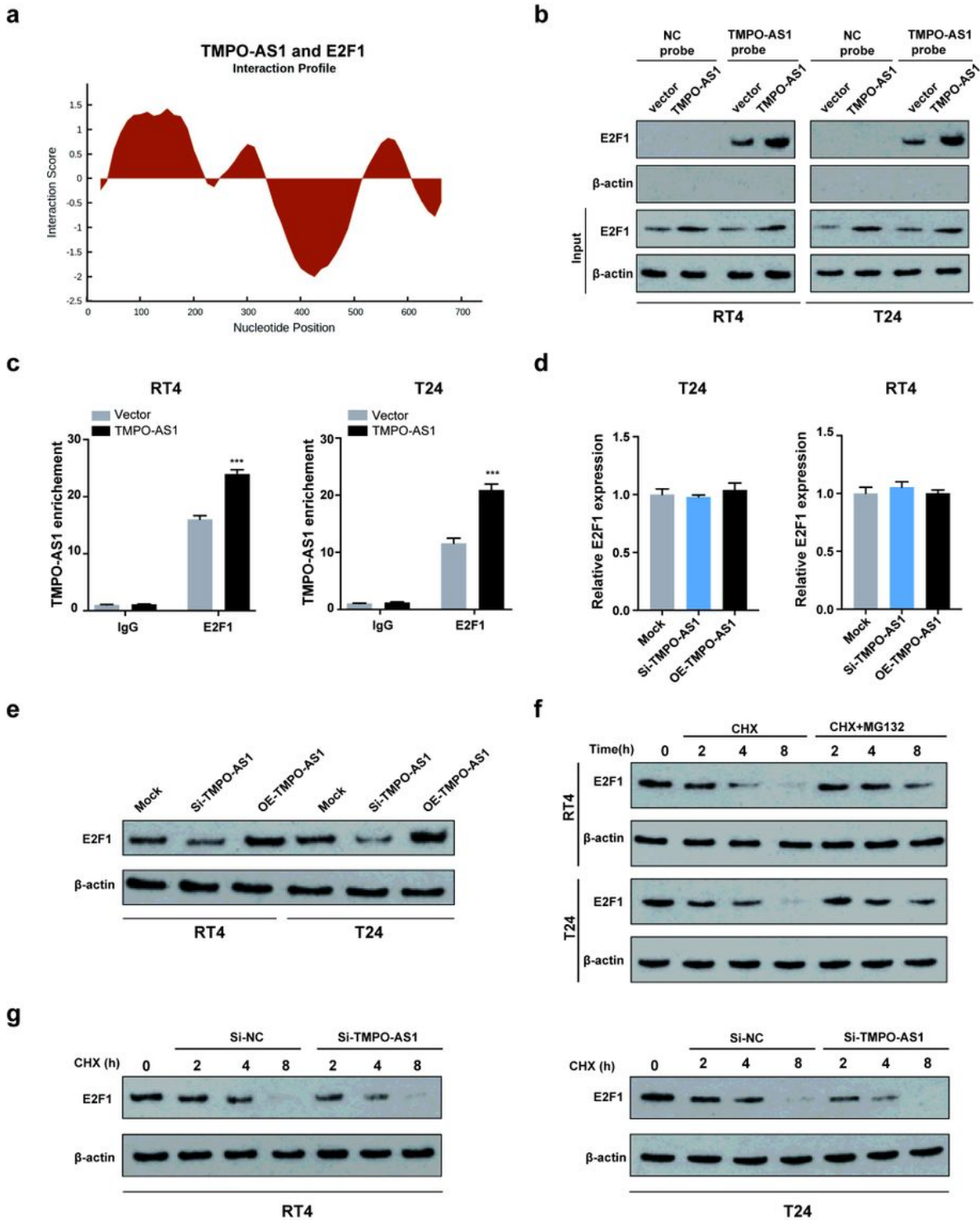
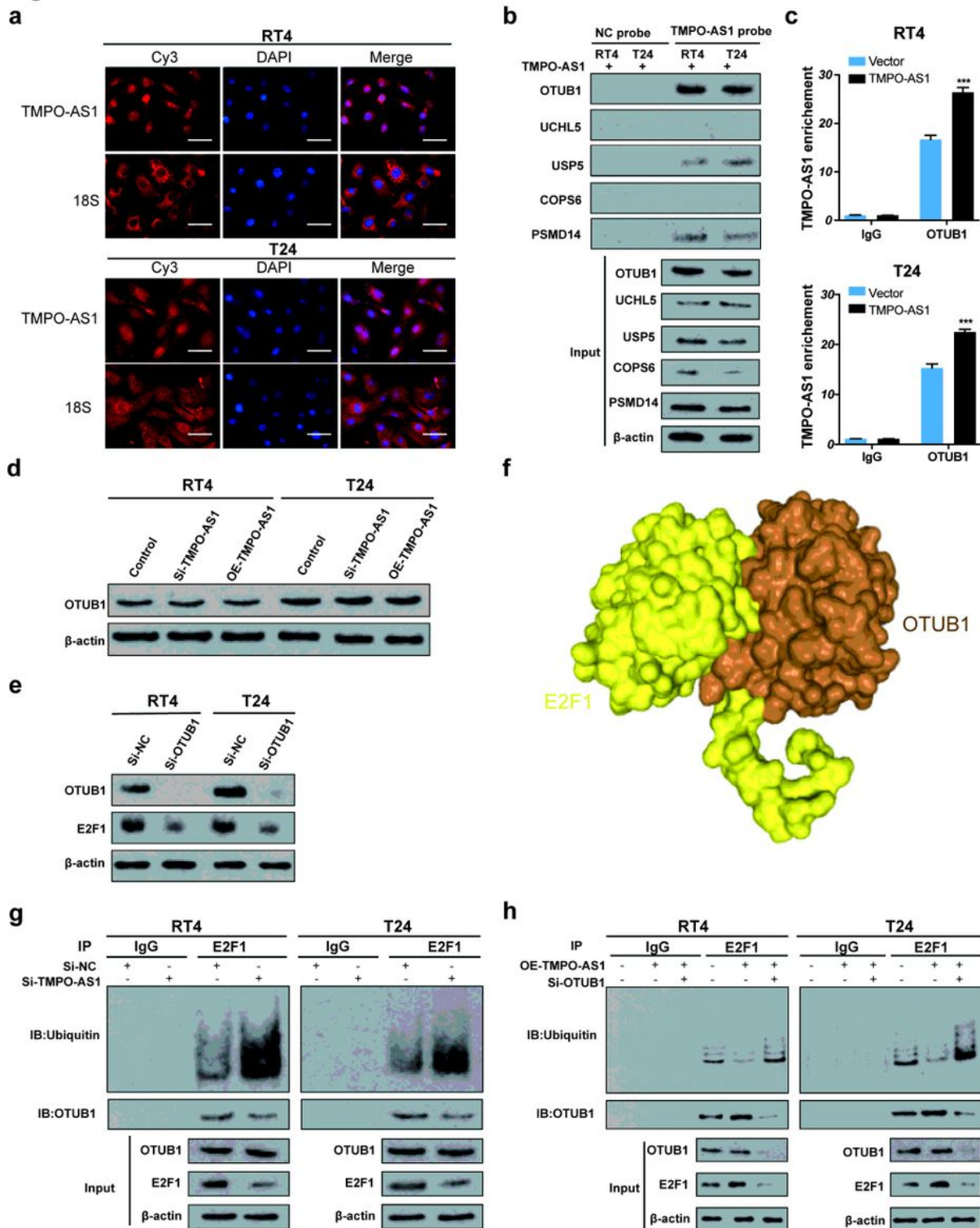


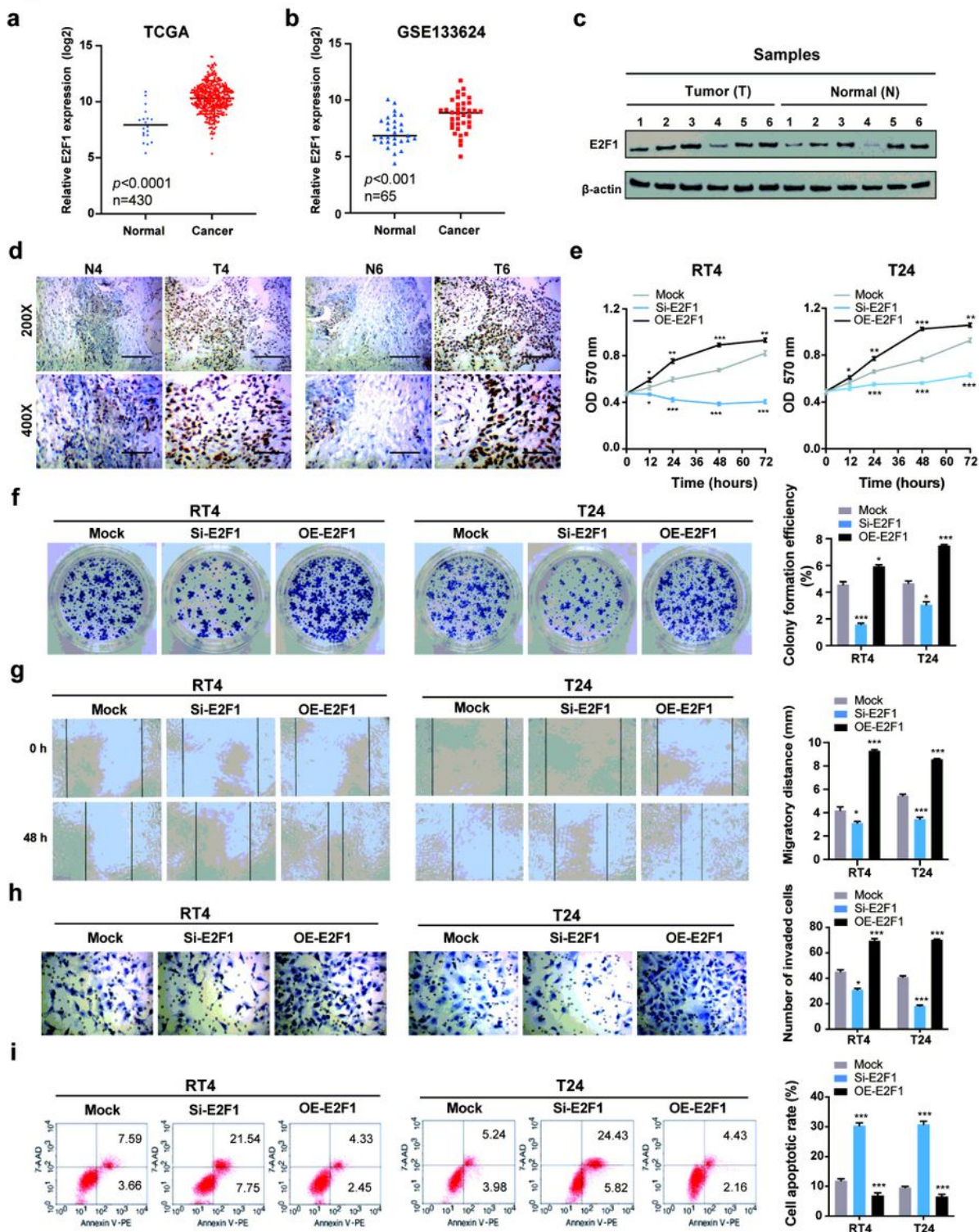
Figure 4

TMPO-AS1 upregulates E2F1 protein levels via the promotion of protein stability. a The interaction between TMPO-AS1 and E2F1 was predicted using catRAPID. b RNA pull-down assay was performed to validate the potential interaction between TMPO-AS1 and E2F1 in RT4 and T24 cells overexpressing TMPO-AS1. c RIP assay was performed to further confirm the interaction between E2F1 and TMPO-AS1, in TMPO-AS1 overexpressing RT4 and T24 cells; IgG was used as a RIP negative control. Error bars represent the mean \pm S.D. from three independent experiments. ***P < 0.001 versus negative control. d E2F1 mRNA expression was assessed using qRT-PCR in TMPO-AS1 silencing or overexpressing BC cells. e E2F1 protein expression was evaluated via western blotting in TMPO-AS1 silencing or overexpressing RT4 and T24 cells. f Western blotting showing proteasome inhibitor MG132 protein increased E2F1 stability in cycloheximide-treated RT4 and T24 cells. CHX, cycloheximide. g Western blotting showing decreased E2F1 stability was observed in TMPO-AS1 knockdown RT4 and T24 cells.

Fig.5**Figure 5**

TMPO-AS1 stabilizes E2F1 via OTUB1-mediated deubiquitination a TMPO-AS1 cellular localization was evaluated using FISH. b RNA pull-down assays demonstrated that OTUB1 was the most likely deubiquitinase binding to TMPO-AS among a group of deubiquitinases (OTUB1, UCHL5, USP5, COPS6, and PSMD14). c RIP assays were performed to validate the interaction between TMPO-AS1 and OTUB1, in the context of TMPO-AS1 overexpressing RT4 and T24 cells; IgG was used as a RIP negative control.

Error bars represent the mean \pm S.D. from three independent experiments. ***P < 0.001 versus negative control. d Western blotting showing TMPO-AS1 silencing had no effect on OTUB1 protein levels in RT4 and T24 cells. e Western blotting showing knockdown of OTUB1 decreased E2F1 protein levels in RT4 and T24 cells. Si- OTUB1, siRNA targeting OTUB1. f HDCK showing E2F1(yellow) and OTUB1(brown) were very likely to bind to each other. g Co-IP assays were performed in control or si-TMPO-AS1 treated RT4 and T24 cells using an anti-E2F1 antibody, followed by western blotting to analyze the ubiquitin levels of E2F1. h RT4 and T24 cells transfected with the empty vector, TMPO-AS1 overexpressing, or along with si-OTUB1 were subjected to immunoprecipitation with anti-E2F1 antibody, followed by western blotting with an anti-ubiquitin antibody.

Fig.6**Figure 6**

E2F1 promotes the proliferation, migration, and invasion, and inhibits the apoptosis of BC cells in vitro. a, b The transcriptional expression of E2F1 was upregulated in BC tissues compared with that in normal tissues based on data retrieved from TCGA and GSE133624. c E2F1 protein expression was assessed via western blotting in six paired BC, and adjacent normal tissue samples. d E2F1 protein expression was also assessed using immunohistochemistry in six paired BC, and adjacent normal tissue samples. e The

MTT was performed to determine the viability/proliferation of E2F1 knockdown and overexpressing RT4 and T24 cells. f The effects of E2F1 knockdown and overexpression on BC cell proliferation were assessed via colony formation assays. g, h The migratory and invasive capacities of E2F1 knockdown and overexpressing RT4 and T24 cells were evaluated via wound healing and transwell assays. i Cell apoptosis was analyzed by flow cytometry. Error bars represent the mean \pm S.D. from three independent experiments. * $P < 0.05$, ** $P < 0.01$, *** $P < 0.001$ versus Mock group (negative control).

Fig.7

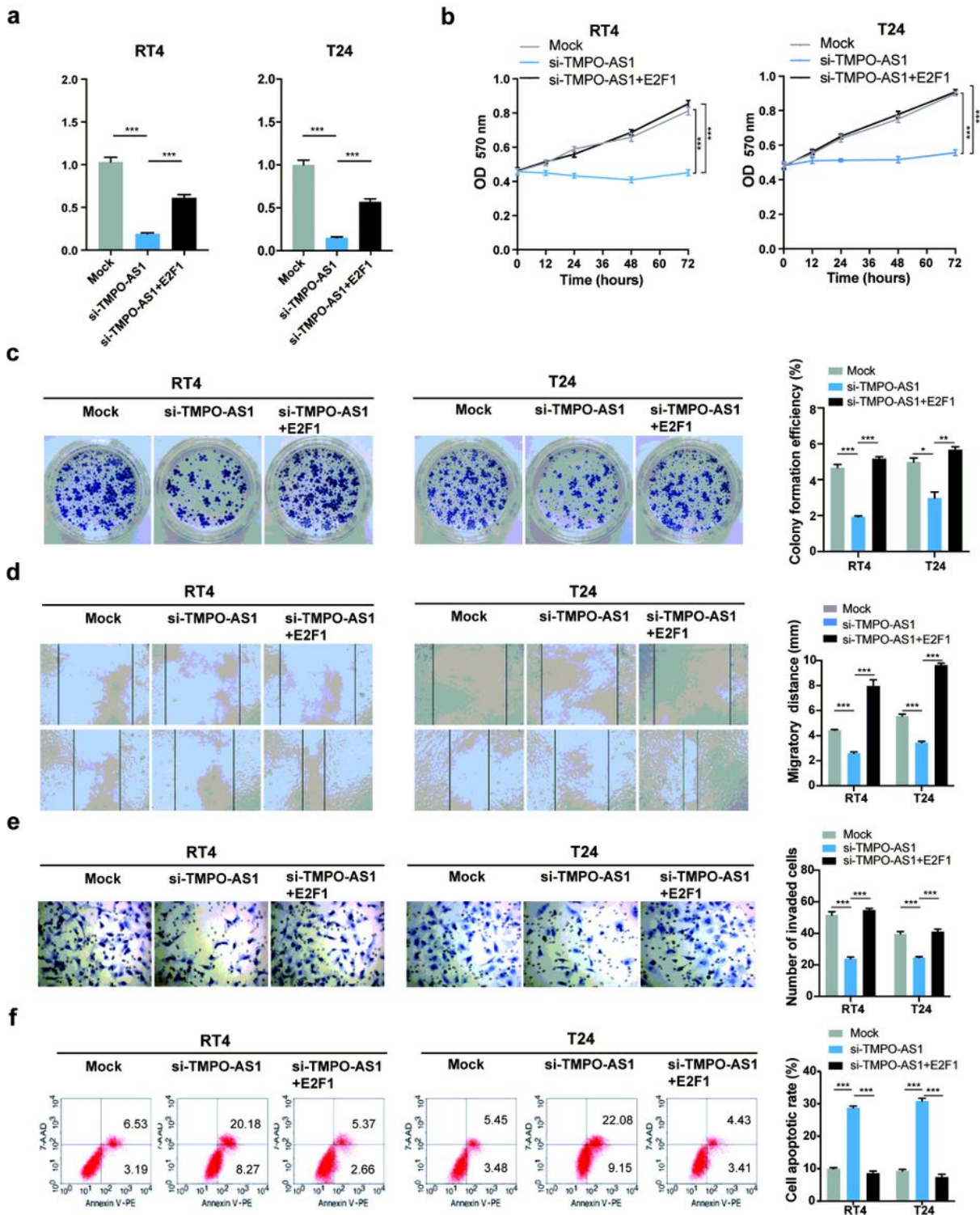


Figure 7

TMPO-AS1 promotes BC malignant phenotypes via E2F1 in vitro. a TMPO-AS1 expression was evaluated using qRT-PCR in RT4 and T24 cells transfected with the empty vector, sh-TMPO-AS1, or co-transfected with sh-TMPO-AS1 and E2F1. b, c MTT and colony formation assays were employed to assess the proliferative ability of transfected cells. d, e Migration and invasion were estimated using wound healing and transwell assays. f The apoptosis in transfected BC cells stained with Annexin V-PE/7-AAD was evaluated via flow cytometry analysis. Error bars represent the mean \pm S.D. from three independent experiments. * $P < 0.05$, ** $P < 0.01$, *** $P < 0.001$.

Fig.8

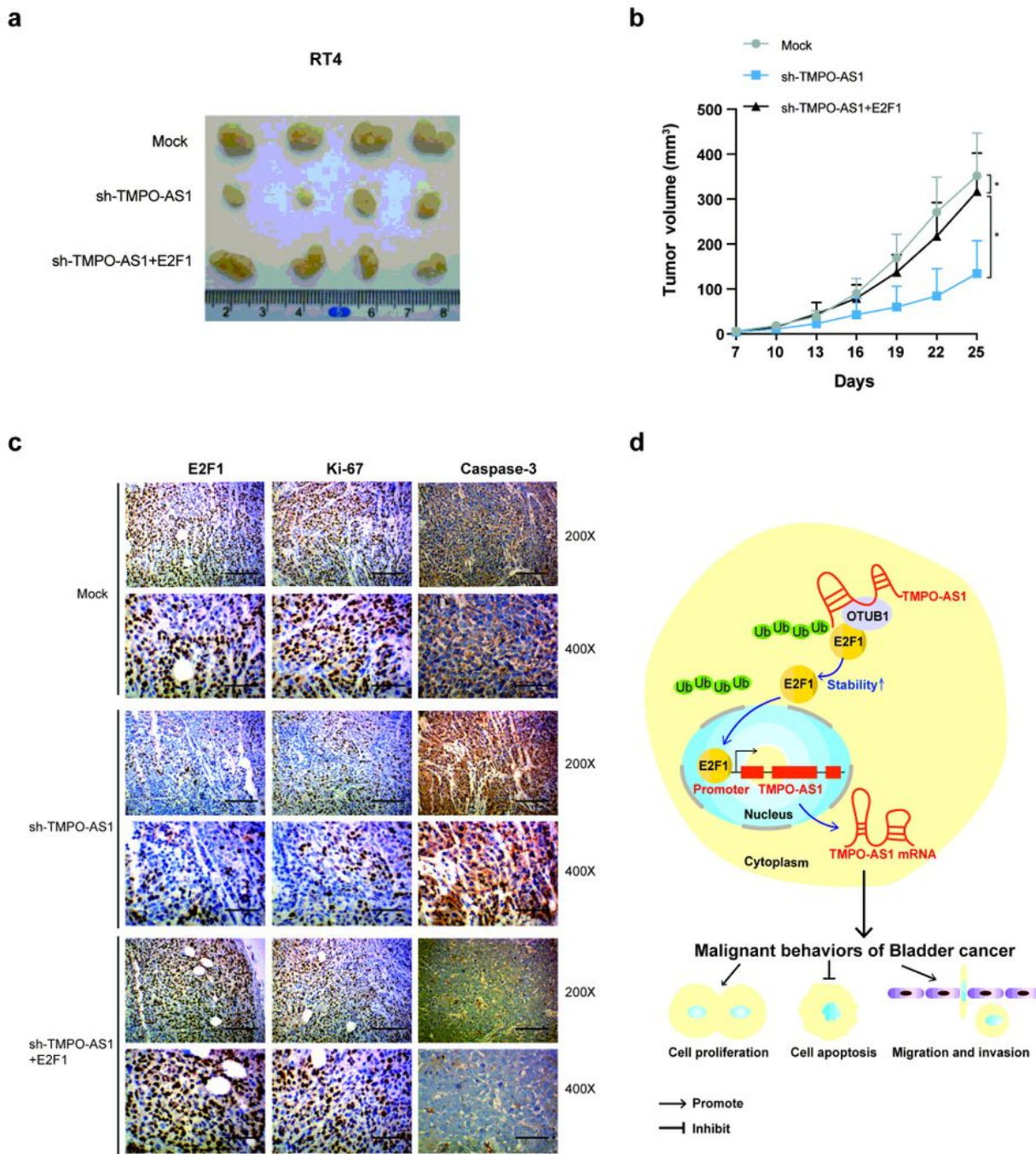


Figure 8

TMPO-AS1 regulates BC growth in vivo via E2F1. a Representative images of the tumor xenografts 25 days after the subcutaneous injection of RT4 cells transfected with the empty vector, sh-TMPO-AS1, and sh-TMPO-AS1 along with E2F1 into the flanks of nude mice. b The tumor volumes were measured every 3 days in the three groups. Three independent experiments were performed. * $P < 0.05$. c The expression of E2F1, Ki-67 and caspase-3 in xenografts was evaluated using immunohistochemistry. Representative images are shown. d A schematic diagram illustrating the role and mechanism of TMPO-AS1 in BC tumorigenesis and progression.

Supplementary Files

This is a list of supplementary files associated with this preprint. Click to download.

- [FigureS2.tif](#)
- [FigureS2.tif](#)
- [TableS3coexpressedgeneswithTMPOAS1.xlsx](#)
- [TableS3coexpressedgeneswithTMPOAS1.xlsx](#)
- [TableS2TFs.docx](#)
- [TableS2TFs.docx](#)
- [FigureS1.tif](#)
- [FigureS1.tif](#)
- [TableS1antibodies.xlsx](#)
- [TableS1antibodies.xlsx](#)
- [Primers.docx](#)
- [Primers.docx](#)